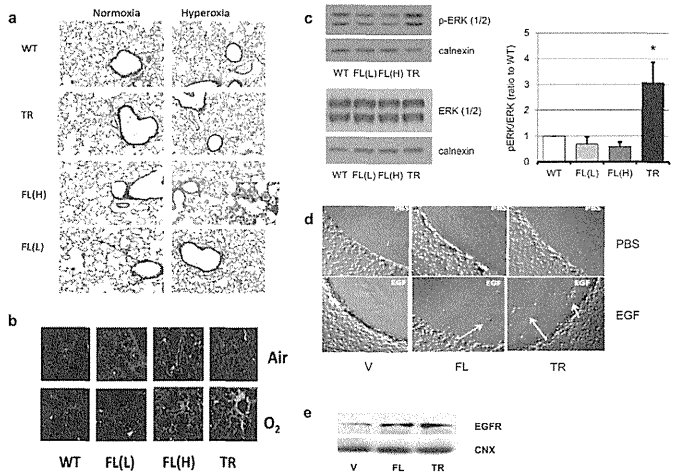

Figure 8. Cell proliferation and tumorigenesis during repair from hyperoxia as adults. (**a**) Representative H&E staining of lung slices from 8 week old HO-1 transgenic mice exposed to hyperoxia as a neonates. Inset: 40×magnification showing abnormal multinucleated intra-alveolar cells. (**b**) Representative p-*ERK* immunosignal in lung slices from 8 week old *HO-1* transgenic mice exposed to hyperoxia as neonates. *P-ERK* is shown in green and DAPI in blue. (**c**) Left-upper panel: representative of 3 western analyses showing total ERK signal in lung homogenates from 8 week old HO-1 transgenic mice exposed to hyperoxia as neonates. Left-lower panel: representative of 3 western analyses showing p-ERK signal in lung homogenates from the same animals. Calnexin serves as the loading control. Right panel: Densitometric evaluation of pERK/ERK ratio from the blots in the left panel. Values are the mean ± SEM of 3 densitometric measurements in each group. *, $p<0.05$ vs WT, FL(L), and FL(H). (**d**) Representative migration of HO-1 infected HO-1 null MEF towards an agarose spot containing EGF. Arrows: migrated cells. (**f**) Representative of 2 western blots for EGFR immunosignal in HO-1 infected HO-1 null MEF cells. Calnexin is the loading control.
doi:10.1371/journal.pone.0090936.g008

suggests that moderate overexpression of HO-1 protein in pulmonary epithelial cells may play a critical role in the resolution of hyperoxia-induced acute lung injury by reducing oxidative stress in type II epithelial cells that are critical targets for hyperoxia-mediated impairment and recovery of postnatal lung development [36]. Interestingly HO activity was not different than WT in this model suggesting that a modelrate change in HO-1 protein, even without activity is sufficient to provide protection. We have previously shown that HO-1 protein even if not catalytically active [37] can alter transcription factor activation and also still provide protection against oxidative stress *in vivo* [13]. This model suggests that the same is true *in vivo*. It could be that the lack of difference in HO activity is due to the fact that the sample represents the whole lung homogenate and that the activity resides only in the type II cells. This remains to be determined.

If moderate overexpression of HO-1 is protective, it seems counterintuitive that further overexpression of HO-1 would worsen hyperoxia-induced lung injury. In fact, this resulted in increased cell proliferation, decreased apoptosis, focal type II cell accumulation, and thickened alveolar walls, contributing to long-term physiological changes in pulmonary function and increased pulmonary densities. The expression of HO-1 is often enhanced in cancer cells, as demonstrated in prostate, brain, pancreatic, and lung cancers as well as several other tissues [38–48]. HO-1 is highly upregulated in rapidly proliferating cells such as in the epithelium within wounded skin or psoriatic lesions. In contrast, HO-1 inhibition reduces the viability of colon carcinoma, acute myeloid leukemia, and hormone-refractory prostate cancer [39,49,50]. It could be that the HO-1-FL(H) with alveolar wall thickness and hypercellularity are prone to malignant transformation. In fact, we observed abnormal cells within the alveoli of HO-1-FL(H) and enhanced migration towards EGF *in vitro* after stable transfection with HO-1-FL cDNA. The abnormal pulmonary densities were predominantly seen after hyperoxic exposure, suggesting that the pro-proliferative and perhaps tumorigenic effects of high HO-1 overexpression were facilitated by hyperoxia. Interestingly, these cells did not bear the typical signature of other lung cancers. It remains to be determined if this would evolve over time. Nevertheless, the maladaptive accumulation of Type II cells also suggests that there is a derangement of the normal repair process which results in Type II to Type I transdifferentiation to maintain proper lung architecture and that this would lead to a persistently abnormal lung architecture.

We were intrigued that we did not see pulmonary densities in the Nuc-HO-1-TR mice because nuclear localization of HO-1 has been associated with malignant transformation and metastasis in several other models [19–21]. Although there were no statistically significant differences in the number of pulmonary densities seen on MRI in Nuc-HO-1-TR, these animals had increased lung p-ERK signaling and MEF stably transfected with Nuc-HO-1-TR cDNA had increased EGFR expression and increased migration towards EGF, further suggesting a tumorigenic potential. Perhaps,

with a longer recovery period, the animals would develop pulmonary foci or abnormal cells.

In the case of the Nuc-HO-1-TR, nuclear HO-1 was increased on a background of endogenous cytoplasmic HO-1. Nevertheless, this model allowed us to evaluate the effects of enhanced nuclear HO-1 on hyperoxic lung injury and was more relevant to the *in vivo* situation in neonates. We have recently shown that PARP is one of the candidate binding partners of HO-1 in the nucleus *in vitro* [23]. Activation of PARP is a cellular response to DNA single strand breaks. Once PARP detects DNA single strand breaks, it binds to the DNA and begins to synthesize a poly PAR chain as a signal for other DNA-repair enzymes, such as X-ray cross-complementing gene 1 [51] and aprataxin polynucleotide kinase phosphatase-like factor [52]. Thereafter, the PAR chains are degraded via PARG [53]. These events facilitate DNA repair. However, the accumulation of PAR could also play a role in PARP-dependent cell death [54,55]. We demonstrated that the interaction of nuclear HO-1 and PARG proteins altered the activity of PARG. We suspect that this led to the persistent DNA damage and subsequent emphysematous phenotype seen on histology and with pulmonary function testing in Nuc-HO-1-TR. This demonstrates that the nuclear HO-1 mediated inhibition of DNA repair in type II cells hinders repair from hyperoxic injury.

In summary, using lung-specific HO-1 transgenic mice, we have demonstrated that there is a beneficial threshold of HO-1 protein overexpression in the lung *in vivo*. Although moderate to low levels of HO-1 expression are beneficial due to inhibition of oxidative damage, high overexpression of HO-1 is harmful due to abnormal cell proliferation and decreased apoptosis, which have both short term and long term-consequences on lung function and structure. Also, overexpression of nuclear HO-1 inhibits repair from hyperoxic lung injury by inhibiting DNA repair, which may predispose the lung to later malignant transformation. A clearer understanding of the nuances of HO-1 cytoprotective effects is important for developing effective therapeutic strategies to prevent lung oxidative injury and tumorigenesis.

Acknowledgments

We thank Dr. Edward Morrisey (University of Pennsylvania) for providing the human SP-C promoter. We are grateful to Dr. Adele Harman (Children's Hospital of Philadelphia) for the production of transgenic mice.

Author Contributions

Conceived and designed the experiments: FN PL GY PAD. Performed the experiments: *FN HG JAM APF MY CB SLW*. Analyzed the data: *FN SS*. Contributed reagents/materials/analysis tools: APF. Wrote the paper: FN PAD. Edited the English text: PAD.

References

1. Gough A, Linden M, Spence D, Patterson CC, Halliday HL, et al. (2013) Impaired lung function and health status in adult survivors of bronchopulmonary dysplasia. Eur Respir J In press.
2. Wong P, Murray C, Louw J, French N, Chambers D (2011) Adult bronchopulmonary dysplasia: computed tomography pulmonary findings. J Med Imaging Radiat Oncol 55: 373–378.
3. Doyle LW, Anderson PJ (2009) Long-term outcomes of bronchopulmonary dysplasia. Semin Fetal Neonatal Med 14: 391–395.
4. Frank L, Bucher JR, Roberts RJ (1978) Oxygen toxicity in neonatal and adult animals of various species. J Appl Physiol 45: 699–704.
5. Hass MA, Massaro D (1987) Differences in CuZn superoxide dismutase induction in lungs of neonatal and adult rats. Am J Physiol 253: C66–70.
6. Hoffman M, Stevens JB, Autor AP (1980) Adaptation to hyperoxia in the neonatal rat: kinetic parameters of the oxygen-mediated induction of lung superoxide dismutases, catalase and glutathione peroxidase. Toxicology 16: 215–225.
7. Ischiropoulos H, Nadziejko CE, Kumar T, Kikkawa Y (1989) Oxygen tolerance in neonatal rats: role of subcellular superoxide generation. Am J Physiol 257: L411–420.
8. Choi AM, Sylvester S, Otterbein L, Holbrook NJ (1995) Molecular responses to hyperoxia in vivo: relationship to increased tolerance in aged rats. Am J Respir Cell Mol Biol 13: 74–82.
9. Dennery PA, Rodgers PA, Lum MA, Jennings BC, Shokoohi V (1996) Hyperoxic regulation of lung heme oxygenase in neonatal rats. Pediatr Res 40: 815–821.
10. Poss KD, Tonegawa S (1997) Reduced stress defense in heme oxygenase 1-deficient cells. Proc Natl Acad Sci U S A 94: 10925–10930.
11. Zhuang T, Zhang M, Zhang H, Dennery PA, Lin QS (2010) Disrupted postnatal lung development in heme oxygenase-1 deficient mice. Respir Res 11: 142.
12. Fernandez-Gonzalez A, Alex Mitsialis S, Liu X, Kourembanas S (2012) Vasculoprotective effects of heme oxygenase-1 in a murine model of hyperoxia-induced bronchopulmonary dysplasia. Am J Physiol Lung Cell Mol Physiol 302: L775–784.
13. Suttner DM, Dennery PA (1999) Reversal of HO-1 related cytoprotection with increased expression is due to reactive iron. FASEB J 13: 1800–1809.
14. Hwang HW, Lee JR, Chou KY, Suen CS (2009) Oligomerization is crucial for the stability and function of heme oxygenase-1 in the endoplasmic reticulum. J Biol Chem 284: 22672–22679.
15. Yoshida T, Sato M (1989) Posttranslational and direct integration of heme oxygenase into microsomes. Biochem Biophys Res Commun 163: 1086–1092.
16. Li Volti G, Ientile R, Abraham NG, Vanella A, Cannavò G, et al. (2004) Immunocytochemical localization and expression of heme oxygenase-1 in primary astroglial cell cultures during differentiation: effect of glutamate. Biochem Biophys Res Commun 315: 517–524.
17. Suttner DM, Sridhar K, Lee CS, Tomura T, Hansen TN, et al. (1999) Protective effects of transient HO-1 overexpression on susceptibility to oxygen toxicity in lung cells. Am J Physiol 276: L443–451.
18. Giordano A, Nisoli E, Tonello C, Cancello R, Carruba MO, et al. (2000) Expression and distribution of heme oxygenase-1 and −2 in rat brown adipose tissue: the modulatory role of the noradrenergic system. FEBS Lett 487: 171–175.
19. Sacca P, Meiss R, Casas G, Mazza O, Calvo JC, et al. (2007) Nuclear translocation of haeme oxygenase-1 is associated to prostate cancer. Br J Cancer 97: 1683–1689.
20. West AR, Oates PS (2008) Subcellular location of heme oxygenase 1 and 2 and divalent metal transporter 1 in relation to endocytotic markers during heme iron absorption. J Gastroenterol Hepatol 23: 150–158.
21. Gandini NA, Fermento ME, Salomón DG, Blasco J, Patel V, et al. Nuclear localization of heme oxygenase-1 is associated with tumor progression of head and neck squamous cell carcinomas. Exp Mol Pathol 93: 237–245.
22. Lin Q, Weis S, Yang G, Weng YH, Helston R, et al. (2007) Heme oxygenase-1 protein localizes to the nucleus and activates transcription factors important in oxidative stress. J Biol Chem 282: 20621–20633.
23. Yang G, Biswasa C, Lin QS, La P, Namba F, et al. (2013) Heme oxygenase-1 regulates postnatal lung repair after hyperoxia: role of b-catenin/hnRNPK signaling. Redox Biol 1: 234–243.
24. Cui Z, Reilly MP, Surrey S, Schwartz E, McKenzie SE (1998) −245 bp of 5′-flanking region from the human platelet factor 4 gene is sufficient to drive megakaryocyte-specific expression in vivo. Blood 91: 2326–2333.
25. Vreman HJ, Stevenson DK (1988) Heme oxygenase activity as measured by carbon monoxide production. Anal Biochem 168: 34–38.
26. Emery JL, Mithal A (1960) The number of alveoli in the terminal respiratory unit of man during late intrauterine life and childhood. Arch Dis Child 35: 544–547.
27. Cooney TP, Thurlbeck WM (1982) The radial alveolar count method of Emery and Mithal: a reappraisal 1 - postnatal lung growth. Thorax 37: 572–579.
28. Yang G, Abate A, George AG, Weng YH, Dennery PA (2004) Maturational differences in lung NF-kappaB activation and their role in tolerance to hyperoxia. J Clin Invest 114: 669–678.
29. Le Rhun Y, Kirkland JB, Shah GM (1998) Cellular responses to DNA damage in the absence of Poly(ADP-ribose) polymerase. Biochem Biophys Res Commun 245: 1–10.
30. Otterbein LE, Soares MP, Yamashita K, Bach FH (2003) Heme oxygenase-1: unleashing the protective properties of heme. Trends Immunol 24: 449–455.
31. Wu M, He YH, Kobune M, Xu Y, Kelley MR, et al. (2002) Protection of human lung cells against hyperoxia using the DNA base excision repair genes hOgg1 and Fpg. Am J Respir Crit Care Med 166: 192–199.
32. Liu Q, Wang B, Yin Y, Chen G, Wang W, et al. (2013) Overexpressions of HO-1/HO-1G143H in C57/B6J mice affect melanoma B16F10 lung metastases rather than change the survival rate of mice-bearing tumours. Exp Biol Med (Maywood) 238: 696–704.
33. Degese MS, Mendizabal JE, Gandini NA, Gutkind JS, Molinolo A, et al. (2012) Expression of heme oxygenase-1 in non-small cell lung cancer (NSCLC) and its correlation with clinical data. Lung Cancer 77: 168–175.

34. Feldser DM, Kostova KK, Winslow MM, Taylor SE, Cashman C, et al. (2010) Stage-specific sensitivity to p53 restoration during lung cancer progression. Nature 468: 572–575.
35. Yee M, Chess PR, McGrath-Morrow SA, Wang Z, Gelein R, et al. (2009) Neonatal oxygen adversely affects lung function in adult mice without altering surfactant composition or activity. Am J Physiol Lung Cell Mol Physiol 297: L641–L649.
36. Yee M, Vitiello PF, Roper JM, Staversky RJ, Wright TW, et al. (2006) Type II epithelial cells are critical target for hyperoxia-mediated impairment of postnatal lung development. Am J Physiol Lung Cell Mol Physiol 291: L1101–L1111.
37. Lin QS, Weis S, Yang G, Zhuang T, Abate A, et al. (2008) Catalytic inactive heme oxygenase-1 protein regulates its own expression in oxidative stress. Free Radic Biol Med 44: 847–55.
38. Schacter BA, Kurz P (1982) Alterations in hepatic and splenic microsomal electron transport system components, drug metabolism, heme oxygenase activity, and cytochrome P-450 turnover in Murphy-Sturm lymphosarcoma-bearing rats. Cancer Res 42: 3557–3564.
39. Alaoui-Jamali MA, Bismar TA, Gupta A, Szarek WA, Su J, et al. (2009) A novel experimental heme oxygenase-1-targeted therapy for hormonerefractory prostate cancer. Cancer Res 69: 8017–8024.
40. Hara E, Takahashi K, Tominaga T, Kumabe T, Kayama T, et al. (1996) Expression of heme oxygenase and inducible nitric oxide synthase mRNA in human brain tumors. Biochem Biophys Res Commun 224: 153–158.
41. Goodman AI, Choudhury M, da Silva JL, Schwartzman ML, Abraham NG (1997) Overexpression of the heme oxygenase gene in renal cell carcinoma. Proc Soc Exp Biol Med 214: 54–61.
42. Sass G, Leukel P, Schmitz V, Raskopf E, Ocker M, et al. (2008) Inhibition of heme oxygenase 1 expression by small interfering RNA decreases orthotopic tumor growth in livers of mice. Int J Cancer 123: 1269–1277.
43. Tsuji MH, Yamagawa T, Iwasa S, Tabuchi K, Onizawa K, et al. (1999) Heme oxygenase-1 expression in oral squamous cell carcinoma as involved in lymph node metastasis. Cancer Lett 138: 53–59.
44. Deininger MH, Meyermann R, Trautmann K, Duffner F, Grote EH, et al. (2000) Heme oxygenase (HO)-1 expressing macrophages/microglial cells accumulate during oligodendroglioma progression. Brain Res 882: 1–8.
45. Torisu-Itakura H, Furue M, Kuwano M, Ono M (2000) Co-expression of thymidine phosphorylase and heme oxygenase-1 in macrophages in human malignant vertical growth melanomas. Jpn J Cancer Res 91: 906–910.
46. McAllister SC, Hansen SG, Ruhl RA, Raggo CM, DeFilippis VR, et al. (2004) Kaposi sarcomaassociated herpesvirus (KSHV) induces heme oxygenase-1 expression and activity in KSHV-infected endothelial cells. Blood 103: 3465–3473.
47. Berberat PO, Dambrauskas Z, Gulbinas A, Giese T, Giese N, et al. (2005) Inhibition of heme oxygenase-1 increases responsiveness of pancreatic cancer cells to anticancer treatment. Clin Cancer Res 11: 3790–3798.
48. Tsai JR, Wang HM, Liu PL, Chen YH, Yang MC, et al. (2012) High expression of heme oxygenase-1 is associated with tumor invasiveness and poor clinical outcome in non-small cell lung cancer patients. Cell Oncol (Dordr) In press.
49. Busserolles J, Megias J, Terencio MC, Alcaraz MJ (2006) Heme oxygenase-1 inhibits apoptosis in Caco-2 cells via activation of Akt pathway. Int J Biochem Cell Biol 38: 1510–1517.
50. Rushworth SA, MacEwan DJ (2008) HO-1 underlies resistance of AML cells to TNF-induced apoptosis. Blood 111: 3793–3801.
51. Okano S, Lan L, Caldecott KW, Mori T, Yasui A (2003) Spatial and temporal cellular responses to single-strand breaks in human cells. Mol Cell Biol 23: 3974–3981.
52. Eustermann S, Brockmann C, Mehrotra PV, Yang JC, Loakes D, et al. (2010) Solution structures of the two PBZ domains from human APLF and their interaction with poly(ADP-ribose). Nat Struct Mol Biol 17: 241–243.
53. Tartier L, Spenlehauer C, Newman HC, Folkard M, Prise KM, et al. (2003) Local DNA damage by proton microbeam irradiation induces poly(ADP-ribose) synthesis in mammalian cells. Mutagenesis 18: 411–416.
54. Koh DW, Lawler AM, Poitras MF, Sasaki M, Wattler S, et al. (2004) Failure to degrade poly(ADP-ribose) causes increased sensitivity to cytotoxicity and early embryonic lethality. Proc Natl Acad Sci U S A 101: 17699–17704.
55. Andrabi SA, Kim NS, Yu SW, Wang H, Koh DW, et al. (2006) Poly(ADP-ribose) (PAR) polymer is a death signal. Proc Natl Acad Sci U S A 103: 18308–18313.

PEDIATRICS INTERNATIONAL Official Journal of the Japan Pediatric Society

Pediatrics International (2015) **57**, 189–192 doi: 10.1111/ped.12584

Brief Report

Drug treatment for bronchopulmonary dysplasia in Japan: Questionnaire survey

Ryo Ogawa,[1] Rintaro Mori,[2] Mayumi Sako,[3] Misao Kageyama,[4] Masanori Tamura[1] and Fumihiko Namba[1]

[1]*Department of Pediatrics, Saitama Medical Center, Saitama Medical University, Saitama,* [2]*Department of Health Policy,* [3]*Division of Clinical Trials, Clinical Research Center, National Center for Child Health and Development, Tokyo and* [4]*Department of Neonatology, Okayama Medical Center, Okayama, Japan*

Abstract Bronchopulmonary dysplasia (BPD) is one of the most common complications in premature infants. Although several different drugs have been developed for BPD, there is a wide variation in the choice of drug used among facilities. The aim of this study was to carry out a survey of the current drugs used to treat BPD in Japan. Questionnaires regarding the current use of drugs for BPD were sent to tertiary neonatal units. The response rate was 80% (77/96). Most units used antenatal steroids and oral diuretics for the prevention and treatment of BPD, respectively. Only 4% used caffeine for prevention, whereas 88% used systemic corticosteroids for treatment. Few units used inhaled anticholinergics and i.v. vitamins for the prevention and treatment of BPD, respectively. It was found that the drugs used to treat BPD vary greatly among institutions. Further research is required to develop evidence-based clinical guidelines for BPD in premature infants.

Key words bronchopulmonary dysplasia, caffeine, drug, questionnaire, steroid.

Bronchopulmonary dysplasia (BPD), also known as a chronic lung disease of infancy, was first described by Northway *et al.* in 1967.[1] Despite ongoing studies to improve neonatal respiratory care, including exogenous surfactant therapy and the use of antenatal steroids, BPD continues to carry a considerable risk of mortality and long-term morbidity. Several devices and strategies, such as nasal continuous positive airway pressure, high frequency oscillatory ventilation, and permissive hypercapnia, have been developed to improve the respiratory outcome of newborns. In addition, several drugs have been used in an attempt to prevent BPD or treat established BPD. Although there is considerable evidence to support the routine use of some drugs, most drug treatment is still individual or institution specific, according to the personal experiences and beliefs of physicians. Therefore, the aim of this study was to survey current practices in Japan regarding the drugs used for the prevention and treatment of BPD and determine whether their use is evidence based.

Methods

A questionnaire was sent to all 96 tertiary neonatal units in Japan. Data were collected between August 2013 and September 2013. Questions were asked on the policies of the neonatal units regarding which drugs were currently used or had been used in the past for the prevention and treatment of BPD. Each question included choice of drug prescribed, which required either a yes or no response together with blank spaces in which the respondents filled in the specific name of a drug. In addition, respondents were given the option of naming drugs not described in the list. BPD was defined as oxygen dependence at 28 days of age. "Preventative therapy" referred to the use of a drug before the diagnosis of BPD on day 28, whereas "treatment" referred to the use of a drug after the diagnosis of BPD.

Correspondence: Fumihiko Namba, MD PhD, Department of Pediatrics, Saitama Medical Center, Saitama Medical University, 1981 Kamoda, Kawagoe, Saitama 350-8550, Japan. Email: nambaf@saitama-med.ac.jp.

Received 7 August 2014; revised 28 October 2014; accepted 17 December 2014.

Results

There was an 80% (77/96) response rate to the questionnaire. The units responding to the questionnaire were distributed evenly from Hokkaido to Okinawa, from the north to the south of Japan, respectively (Fig. 1). A total of 87% of the units used antenatal steroids to prevent BPD, which is known to prevent respiratory distress syndrome (RDS) by accelerating fetal lung maturation (Fig. 2a). Among the antenatal steroids used to prevent BPD, betamethasone was given in 97% of the units, whereas dexamethasone was used only in 3% (Fig. 3a). Oral diuretics, most commonly furosemide and spironolactone, were used in 84% of the units for the treatment of BPD (Fig. 2b). Several drugs were used in <10% of the units, such as β-stimulators and anticholinergic agents for the prevention of BPD, and protease inhibitors and antioxidants for the treatment of BPD. These were considered to be institution-specific practices without any evidence (Fig. 2). Oral xanthine derivatives were used for the prevention of BPD in 42% of the units, but caffeine therapy

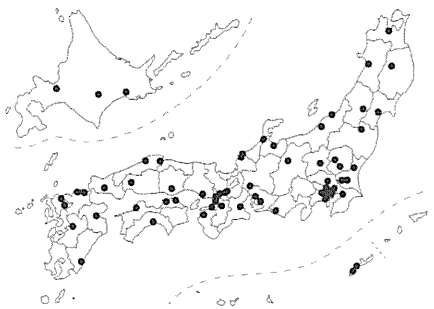

Fig. 1 Tertiary neonatal units in Japan that responded to the questionnaire. Response rate was 80% (77/96).

was offered in only 13% of these units, and theophylline and aminophylline were used in 72% and 16%, respectively (Fig. 2). Vitamin A was used for the prevention of BPD in only 8% of the units (Fig. 2a). The use of early (<28 days of life) and delayed/late (≥28 days of life) systemic corticosteroids (i.v. or p.o.) occurred in 35% and 88% of units, respectively (Fig. 2). Hydrocortisone was used as an early systemic corticosteroid in 70% of units, whereas dexamethasone was used in 21% after evidence had been established that more adverse neurodevelopmental outcomes occur following early systemic dexamethasone therapy (Fig. 3b).[2] Delayed/late systemic corticosteroids, including hydrocortisone (85%) and dexamethasone (53%), were used to treat BPD in 89% of the units (Figs 2b, 3d).

Discussion

This is the first Japanese survey of the drugs used to prevent and treat BPD. The response rate was generally good.

This survey showed that most units use antenatal corticosteroids to prevent BPD. The use of a single course of corticosteroids in a mother who is in preterm labor to accelerate the maturation of the surfactant system in the fetal lungs is considered safe. Although this reduces mortality and the risk of RDS, there is no evidence that it reduces the risk of BPD, probably because of an increase in survival.[3] The use of multiple courses of antenatal corticosteroids significantly increased the risk of BPD, but systematic review comparing the use of multiple courses with a single course did not show any difference in the risk of BPD.[3] Although there is no evidence to support the efficacy of antenatal corticosteroid therapy in BPD, antenatal corticosteroids are used to prevent BPD in Japan. This may be because RDS is one of the most common risk factors for the development of BPD.

Caffeine is a methylxanthine that is commonly used to treat apnea of prematurity.[4] Methylxanthines reduce the frequency of apnea of prematurity and the need for mechanical ventilation during the first 7 days of treatment.[5] A recent large randomized controlled trial followed the primary outcome of long-term neurodevelopment, and secondary outcome of short-term BPD rate in infants with birthweight 500–1250 g.[5] A total of 36% of the infants in the caffeine-treated group had BPD compared with 47% in the placebo group.[5] The mechanism by which caffeine decreases the incidence of BPD, however, remains unknown. Nevertheless, current evidence supports the use of caffeine for the treatment of apnea of prematurity and also suggests that it exerts secondary benefits including a reduction in the rate of BPD. Despite the utility of caffeine for the prevention of BPD, only 4% of the units that responded to the survey in the current

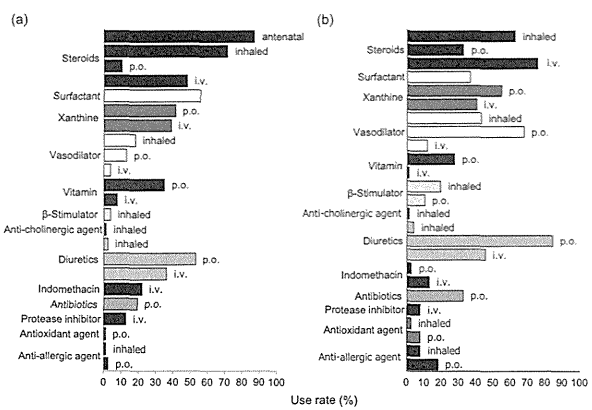

Fig. 2 Drugs for (a) prevention (i.e. before diagnosis on day 28) and (b) treatment (i.e. after diagnosis on day 28) of bronchopulmonary dysplasia in Japan.

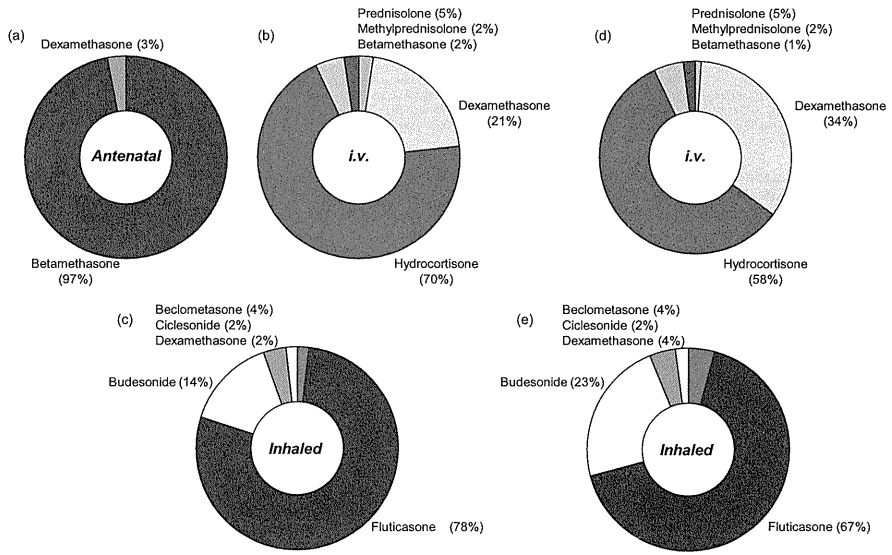

Fig. 3 Steroids for (a–c) prevention (before diagnosis on day 28) and (d,e) treatment (after diagnosis on day 28) of bronchopulmonary dysplasia in Japan.

study used caffeine to prevent the development of BPD. This is because caffeine citrate is not approved for use in Japan, even though it is approved in at least 38 countries worldwide, including the USA and European countries. Caffeine citrate is only one drug that can be used in the treatment of apnea of prematurity listed in "WHO Model List of Essential Medicines for Children".[6] Caffeine citrate is currently under review for drug registration in Japan and is likely to be approved for use in 2014. A reduction in the rate of BPD is expected after the use of caffeine citrate has been approved.

A Cochrane meta-analysis of randomized controlled trials to evaluate the effects of early dexamethasone treatment (<8 days after birth) on the incidence of BPD, found that steroids facilitated extubation and decreased the incidence of BPD.[2] Adverse effects, however, such as hyperglycemia, gastrointestinal perforation, hypertension, infection, steroid-induced cardiomyopathy, and long-term neurodevelopmental effects including cerebral palsy were observed.[2] In the present survey, dexamethasone was used for the prevention of BPD in 30% of cases that involved systemic corticosteroids. Although it is unknown whether dexamethasone was used early (within 7 days of birth) in those patients, 30% still appears to be a high use rate. Secondary questionnaire are required to determine the date that dexamethasone was given, and stern warnings should be issued to the units that administered dexamethasone soon after delivery.

A small number of units used inhaled anticholinergic, oral expectorants, and inhaled disodium cromoglycate for the prevention of BPD, whereas i.v. vitamin, inhaled anticholinergic, and inhaled antioxidant were used for the treatment of BPD. Most of these may represent cases of drug misuse because of a lack of evidence for the efficacy of these agents in BPD or because of their very institution-specific use; therefore, appropriate clinical studies or guidelines are required.

Conclusion

This is the first Japanese survey of the drugs used to prevent and treat BPD, and it achieved a good response rate. The present survey provides information on the heterogeneity of treatment practices for BPD in the participating centers. The survey confirms the misuse of some drugs, and thereby highlights the importance of the formulation and dissemination of evidence-based guidelines for the prevention and treatment of BPD.

Acknowledgments

Dr Namba is supported by Young Investigator Grant from Kawano Masanori Memorial Public Interest Incorporated Foundation for Promotion of Pediatrics, Saitama Medical University Internal Research Grant from Saitama Medical University, and Health Labour Sciences Research Grant, "Studies to elucidate the pathogenesis and long-term outcomes of low birthweight infants" from the Ministry of Health Labour and Welfare.

References

1 Northway WH, Rosan RC, Porter DY. Pulmonary disease following respirator therapy of hyaline-membrane disease. Bronchopulmonary dysplasia. *N. Engl. J. Med.* 1967; **276**: 357–68.
2 Doyle LW, Ehrenkranz RA, Halliday HL. Early (<8 days) postnatal corticosteroids for preventing chronic lung disease in preterm infants. *Cochrane Database Syst. Rev.* 2014; (5): CD001146.
3 Crowley P. Prophylactic corticosteroids for preterm birth. *Cochrane Database Syst. Rev.* 2000; (2): CD000065.
4 Henderson-Smart DJ, Steer P. Methylxanthine treatment for apnea in preterm infants. *Cochrane Database Syst. Rev.* 2001; (3): CD000140.
5 Schmidt B, Roberts RS, Davis P *et al.* Caffeine therapy for apnea of prematurity. *N. Engl. J. Med.* 2006; **354**: 2112–21.
6 *WHO Model List of Essential Medicines for Children*, 4th edn. 2013. [Cited April 2013.] Available at: http://www.who.int/medicines/publications/essentialmedicines/en/.

Journal of Human Genetics (2014) 59, 326–331

www.nature.com/jhg

ORIGINAL ARTICLE

Compilation of copy number variants identified in phenotypically normal and parous Japanese women

Ohsuke Migita[1,11], Kayoko Maehara[1,11], Hiromi Kamura[1], Kei Miyakoshi[2], Mamoru Tanaka[3], Seiichi Morokuma[4], Kotaro Fukushima[4], Tomihiro Shimamoto[5], Shigeru Saito[6], Haruhiko Sago[7], Keiichiro Nishihama[8], Kosei Abe[1], Kazuhiko Nakabayashi[1], Akihiro Umezawa[9], Kohji Okamura[10] and Kenichiro Hata[1]

With increasing public concern about infertility and the frequent involvement of chromosomal anomalies in miscarriage, analyses of copy number variations (CNVs) have been used to identify the genomic regions responsible for each process of childbearing. Although associations between CNVs and diseases have been reported, many CNVs have also been identified in healthy individuals. Like other types of mutations, phenotypically indefinite CNVs may have been retained and accumulated during anthropogenesis. Therefore to distinguish causative variants from other variants is a formidable task. Furthermore, because previous studies have predominantly focused on European and African populations, comprehensive detection of common Asian CNVs is eagerly awaited. Here, using a high-resolution genotyping array and samples from 411 Japanese women with normal parity without significant complications, we have compiled 1043 copy number variable regions. In total, the collected regions cover 164 Mb, or up to 0.5% of the genome. The copy number differences in these regions may be irrelevant not only to infertility but also to a wide range of diseases. The utility of this resource in reducing the candidate pathogenetic variants, especially in Japanese subjects, is also demonstrated.
Journal of Human Genetics (2014) **59**, 326–331; doi:10.1038/jhg.2014.27; published online 1 May 2014

INTRODUCTION

The advent of new technologies has allowed the identification of structural variants that have a more significant impact on human diversity than does the entire set of single-nucleotide polymorphisms (SNPs). Copy number variations (CNVs) are one such type of structural variant and constitute the largest proportion of genomic variations.[1–3] CNVs result from the duplication or deletion of a DNA segment and are commonly observed in human genomes.[4–7] When a genomic event results in a CNV, not only the copy number of a gene can be altered but also its genic sequences. Therefore, CNVs can cause disease or contribute to disease susceptibility,[8–10] and they have been compiled in several databases for public use.[9–11]

Although a number of deleterious changes may have been negatively selected during human evolution, it is likely that phenotypically neutral changes have been retained, transmitted and accumulated over generations. Increasing numbers of CNVs are found in phenotypically normal human individuals.[1] Accordingly, each ethnic group tends to have distinct features in terms of the positions, copy numbers and frequencies of their CNVs, and it is possible that fixed CNVs have contributed to ethnic differences in phenotypic variations and disease susceptibility.[12–15] Therefore, it is important to have a list of CNVs for each ethnic group, especially for medical purposes. However, the number of reported CNVs from Asian populations is small compared with those of Europeans and Africans. Extensive examination of Asian CNVs is eagerly awaited by Asian researchers.

The compilation of nonpathogenic variations, in addition to disease-related variations, is also important for a better understanding of the genetic landscape of the human genome. Data sets including both these sorts of variations should be helpful in pinpointing causative mutations. Even when we search for variations using patient samples, most of the variations identified would be normal polymorphisms, together with a few pathogenic mutations. Although we can consider most of the available variation data nonpathogenic, it is difficult to know which variations are pathogenic. Therefore, the collection of data from normal controls is essential. To investigate phenotypically 'normal' samples in this study, we considered reproduction and child development, and chose parous Japanese women, who had experienced normal pregnancies and deliveries.

Although the origin of the Japanese population remains controversial, the last major migration to the Japanese Archipelago is thought to have occurred approximately 2000 years ago.[16,17] The population has been mixed well with various Asian ethnic groups during previous migrations, but has remained relatively isolated for 2000 years. However, although the current population of Japan is 127 million, far fewer CNVs have been documented in Japanese samples than in Europeans. Compiling a list of Japanese CNVs is also important from the perspective of medical science in Japan.

[1]Department of Maternal–Fetal Biology, National Research Institute for Child Health and Development, Tokyo, Japan; [2]Department of Obstetrics and Gynecology, School of Medicine, Keio University, Tokyo, Japan; [3]Department of Obstetrics and Gynecology, St Marianna University School of Medicine, Kanagawa, Japan; [4]Department of Obstetrics and Gynecology, Graduate School of Medical Sciences, Kyushu University, Fukuoka, Japan; [5]Department of Obstetrics and Gynecology, Miyazaki Prefectural Miyazaki Hospital, Miyazaki, Japan; [6]Department of Obstetrics and Gynecology, University of Toyama, Toyama, Japan; [7]Department of Maternal–Fetal and Neonatal Medicine, National Center for Child Health and Development, Tokyo, Japan; [8]Illumina KK, Tokyo, Japan; [9]Department of Reproductive Biology and Pathology, National Research Institute for Child Health and Development, Tokyo, Japan and [10]Department of Systems BioMedicine, National Research Institute for Child Health and Development, Tokyo, Japan
[11]These authors contributed equally to this work.
Correspondence: Dr K Okamura or Dr K Hata, Department of Maternal–Fetal Biology, National Research Institute for Child Health and Development, 2-10-1 Okura, Setagaya Ward, Tokyo 157-8535, Japan.
E-mail: okamura-k@ncchd.go.jp or hata-k@ncchd.go.jp
Received 27 September 2013; revised 21 March 2014; accepted 26 March 2014; published online 1 May 2014

MATERIALS AND METHODS

Subject recruitment and SNP genotyping with a high-resolution microarray

We examined 411 unrelated Japanese women who had had one or more normal parities, with no significant abnormalities in any of their pregnancies, deliveries or neonates. Ethical approval was also obtained from each review board of the hospitals that participated in the study. The informed consent of all the subjects was obtained. To avoid cell-culture-induced chromosomal rearrangements, genomic DNAs were extracted directly from blood using the QIAsymphony DNA Midi Kit (Qiagen, Venlo, The Netherlands) with the QIAsymphony SP instrument and analyzed with a high-resolution SNP-based genotyping microarray, HumanOmni2.5-8 BeadChip (Illumina, San Diego, CA, USA). Only data that met the quality control guidelines of the manufacturer were used for further analyses.

Identification of CNVs and CNVRs

Two distinct algorithms were used to maximize the specificity of our CNV calling: a likelihood-based method with CNVPartition version 3.2.0 (http://www.illumina.com/software/illumina_connect.ilmn) and a hidden Markov method with PennCNV version (27 August 2009).[18] The parameters applied with these tools were referred to those typically used by many research groups (at least three consecutive probes to define a CNV, using the GC wave adjustment option, etc.). These programs computed confidence scores that can be used to filter out CNV regions that are likely to be false positives. However, we should note that the two programs calculated the scores in different ways, with different scales. To minimize false positives, we first chose only CNVs with high confidence scores; that is, more than 100 with CNVPartition, and selected copy number variable regions (CNVRs) that overlapped those called by PennCNV for at least 80% of their lengths. For PennCNV, we generated a list of B allele frequencies using a collection of signal intensities for 47 samples from HapMap Japanese in Tokyo with the compile_pfb script (Figure 1a).

Multiplex PCR assay

Multiplex polymerase chain reaction (PCR) assay was used to confirm regions that had been called homozygously deleted. The reactions were performed with both a control primer pair that generated a 296-bp fragment and a test primer pair that amplified a target region. The thermal cycling conditions were initial denaturation at 95 °C for 2 min, followed by 35 cycles of denaturation at 95 °C for 30 s, annealing at 60 °C for 30 s and extension at 72 °C for 30 s, and a final extension at 72 °C for 3 min. Detailed information on these primers is given in Supplementary Table S3.

RESULTS

Genetic ancestry of the subjects

First, the population structure was inferred with the Structure software (http://pritchardlab.stanford.edu/structure.html) to confirm the Japanese ancestry of the subjects.[19] A cluster analysis of our samples together with the sequences of 499 HapMap individuals from three ancestral populations (European, African and Asian) was performed using 1959 unlinked tag SNPs on chromosome 21. The expected ancestry of all the subjects was confirmed with a minimum coefficient of 0.85. We also performed a principal components analysis with the pca.jar program (Biobank Japan project; http://genome-analysis.src.riken.jp/PCP/). The results indicated that all but one subject were derived from the main islands of Japan and that the remaining singleton was Ryukyuan.[20]

Characterization of CNVs and CNVRs

The CNVPartition software (Illumina) identified 26 150 candidate regions as CNVs. We then used another program, PennCNV,[18] which is based on an integrated hidden Markov algorithm, to maximize the specificity of the analysis. If a candidate CNV was also supported by PennCNV for at least 80% of its length, it was retained. In this way,

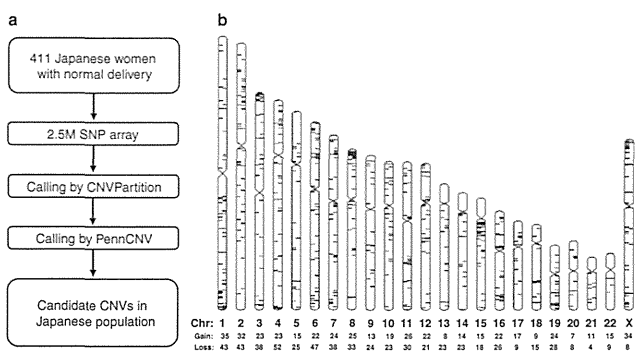

Figure 1 (**a**) Data processing flow. The initial 26 150 regions identified with CNVPartition were validated with PennCNV. (**b**) Chromosomal distribution of the CNVRs. Each CNVR is shown by a horizontal bar. Gain- and loss-type CNVs are distinguished by bars on the left and right, respectively. The numbers of each type of CNV are also shown, and are drawn with Idiographica (http://www.ncrna.org/idiographica/). CNV, copy number variation; CNVR, copy number variable regions.

Table 1 Comparison of the CNVRs with those reported in other studies and in the DGVs

	Present study	*McCarroll et al.*[21]	*Conrad et al.*[22]	*Koike et al.*[23]	*DGV Jul. 2013*
CNVs reported	1043	592	1768	169	202 430
CNVs spanning our data	1043	88 (71/1043)[a]	156 (112/1043)[a]	37 (45/1043)[a]	30 322 (1033/1043)[a]
Number of samples	411 Japanese females	45 HapMap JPT	45 HapMap JPT	57 Japanese females and 123 Japanese males	Collective (including non-Japanese samples)
Experimental method	SNP array (Illumina HumanOmni2.5-8 BeadChip)	SNP array (Affymetrics Genome-Wide Human SNP Array 6.0)	Custom CGH array (NimbleGen and Agilent)	SNP array (Affymetrics Genome-Wide Human SNP Array 6.0)	N/A
CNV calling	CNVPartition and then PennCNV	Birdseye and custom program	Custom program	PennCNV	N/A

Abbreviations: CNV, copy number variations; CNVR, copy number variable region; DGV, database of genomic variants; JPT, Japanese in Tokyo; N/A, not available; SNP, single-nucleotide polymorphism.
[a]The number of CNVRs overlapped with those in the present study is indicated within parentheses.

Table 2 CNVRs overlapping between the Japanese and other populations

Population	*Sample size*	*Reported CNVRs*	*Frequency of overlapping regions among studies*[a]
Japanese (present study)	411	1043	—
Korean[24]	100	576	10% (106/1043)
Tibetan[14]	29	139	4.9% (51/1043)
Chinese[13] (Han, Tibetan and five other ethnic group)	155	1440	17% (173/1043)
Han Chinese[13]	80	1407	17% (175/1043)
Swiss[25]	717	917	16% (163/1043)
Rwandan[25] (sub-Saharan African)	450	1185	14% (141/1043)
HapMap[26] (mixed)	112	3262	13% (134/1043)

Abbreviation: CNVR, copy number variable regions.
[a]Number of overlapped CNVRs is indicated within parentheses.

Table 3 List of genes lying within a homozygously deleted region

No.	*Coordination*	*Frequency*	*Suffered gene*		
1	Chr 1: 161 570 803–161 644 281*	2/411	*FCGR3B*	*FCGR2B*	
2	Chr 2: 111 884 593–111 886 246*	3/411	*BCL2L11*		
3	Chr 4: 69 367 146–69 489 473*	302/411	*UGT2B17*		
4	Chr 5: 180 377 470–180 424 820*	32/411	*BTNL3*		
5	Chr 6: 32 551 892–32 555 728	2/411	*HLA-DRB1*		
6	Chr 7: 115 584 568–115 593 688*	1/411	*TFEC*		
7	Chr 7: 141 761 027–141 795 404*	6/411	*MGAM*		
8	Chr 11: 18 949 220–18 961 743	1/411	*MRGPRX1*		
9	Chr 19: 41 350 895–41 379 321*	10/411	*CYP2A6*		
10	Chr 19: 43 590 229–43 772 302	86/411	*PSG5*	*PSG4*	*PSG9*
11	Chr 19: 46 622 776–46 636 139*	3/411	*IGFL3*		
12	Chr 19: 52 132 392–52 150 601*	114/411	*SIGLEC5*		

Abbreviation: PCR, polymerase chain reaction.
Asterisk indicates a homozygously deleted region validated by PCR.

we identified 6871 CNVs and 1043 regions with variable copy numbers from 411 Japanese individuals, with an average of 16.7 CNVs per diploid genome (Supplementary Table S1). Detailed information on all the SNP probes used for the CNV calls is tabulated (Supplementary Table S2). The mean length of the CNVs was 79.9 kb, ranging from 169 bases to 2.27 Mb. These 6871 CNVs corresponded to 1043 CNVRs (588 losses and 455 gains). Figure 1 shows the chromosomal distribution of the observed CNVRs. The total length of all of these CNVRs was 163 720 kb, which is equivalent to 0.5% of the whole human genome. The CNVRs can be divided into gain regions and loss regions, depending on whether their copy numbers have increased or decreased. Of the 1043 regions identified, 1033 overlap the latest database of genomic variants (DGVs) (released on 23 July 2013) reported at the DGV. More than half the CNVRs, including 72% of the gain CNVRs and 36% of the loss CNVRs, intersect RefSeq gene loci.

As far as we know, three studies have examined the Japanese population with array-based methods: two of them used samples from HapMap and the other used healthy individuals.[21–23] These results are summarized with our data set (Table 1). Although those three studies had together already reported 82 regions, more than half the regions reported in the present study were not detected by them. It is probable that the higher resolution of our analysis and our larger sample size allowed us to detect additional CNVRs. Depending on the types of platform used, array-based CNV studies occasionally show discrepancies in the regions of CNVs.[21,22] Differences in the array architectures, scanning machines and calling algorithms could affect the final data sets. Using reported CNV data from SNP arrays, we counted the overlapping regions among studies that focused on other populations or HapMap data[13,14,24–26] (Table 2). The similarities among these studies are comparable, but our results suggest a greater similarity between the Japanese and Chinese populations.

Homozygous deletions found in parous Japanese women

In our study, 1628 homozygous deletions that could affect 112 RefSeq gene loci were called in a total of 822 chromosomes. Although the CNV analysis was unable to determine the precise breakpoints, our data indicate that some exonic sequences are disrupted by homozygous deletions (Table 3). Using multiplex PCR with both control and test primer pairs, we confirmed the null genotypes caused by deletions (Supplementary Figure S1 and Supplementary Table S3). Five genes, *FCGR3B*, *FCGR2B*, *UGT2B17*, *HLA-DRB1* and *CYP2A6*, are described as disease related in the OMIM database. The *FCGR3*, *FCGR2B* and *HLA-DRB1* genes have roles in the immune system. *FCGR3B* and *FCGR2B* encode the crystallizable region of immunoglobulin G. Several studies have shown that a low copy number at the *FCGR3B–FCGR2B* locus is associated with a susceptibility to systemic lupus erythematosus in the Caucasian population,[27–29] but not in the Chinese population.[28] *UGT2B17* encodes a protein that belongs to the family of UDP-glucuronosyltransferases enzymes, which catalyzes the glucuronidation of steroid hormones. A case–control study of osteoporosis-related fracture suggested that a CNV at the *UGT2B17* locus contributes to osteoporosis.[30] Jakobsson *et al.*[31] found that its null genotype was more common in Koreans (67%) than in Swedish (9%). Our array results also showed a high frequency (74%) of the null genotype. The CYP2A6 protein metabolizes nicotine and coumarin in the liver. The lack of a *CYP2A6* gene may affect nicotine levels in individuals and probably has a protective effect against tobacco dependence.[32] Another study reported that the frequency of homozygotes for the *CYP2A6* gene deletion was lower in Japanese lung cancer patients than in control samples.[33] Except for *HLA-DRB1*, these disease-related genes have been reported to be frequently deleted in Asian populations.[25,34–36] Because we limited our samples to parous women only, it is unlikely that the CNVRs identified in the present study are related to human reproduction.

DISCUSSION

In the present study, we compiled a catalog of copy number variable regions identified in phenotypically normal Japanese samples, especially those with a history of full-term pregnancy and deliveries without major complications. The data set will be useful in the search for novel or rare CNVs that increase the individual's susceptibility to congenital diseases and complications during pregnancy. It is unlikely that the newly identified CNVs are related to infertility or miscarriage. CNVs in parous women without complications have never before

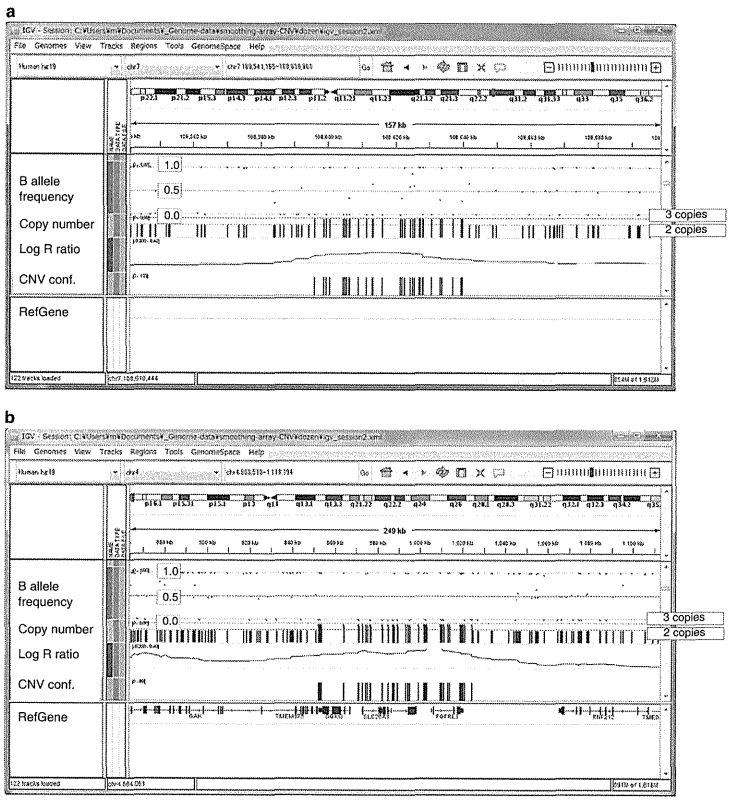

Figure 2 (**a**) A copy number variation (CNV) located on chromosome 7. The panel shows the region at nucleotides 108 541 155–108 698 960 in hg19. This CNV was called with high-intensity probes. The B allele frequencies (BAFs) were separated into four levels, which corresponded to AAA, AAB, ABB and BBB, respectively. (**b**) Another CNV located in the subtelomeric region on chromosome 4. The panel shows the region at nucleotides 863 513–1 113 194. Despite high-intensity probes used, as in the example shown above, the four levels of BAFs were not observed, suggesting that the call might be implausible. Such CNVs tended to be called in G+C-rich regions; for example, 58% G+C content in this case. The snapshot was made with the IGV program (http://www.broadinstitute.org/igv/). A full color version of this figure is available at *Journal of Human Genetics* online.

been investigated. Although the copy numbers of these regions were not thoroughly validated with other methods; such as, quantitative PCR, according to DGV, most of the CNVRs identified here have been reported in previous studies, indicating that they should be observed by other methods or techniques. Because our identification strategy was based on a microarray technique, it is inevitable that errors would have occurred. Besides routine data processing, we also carefully curated the data by examining the B allele frequencies and signal intensities (log *R* ratio) for each CNVR using the GenomeStudio software (Illumina) (Figure 2). We found that many implausible calls were situated in regions with high G + C contents; for example, in subtelomeric regions. All of them were copy number gain-type CNVs rather than copy number loss-type CNVs. Although further research is required, it is important to note that CNVRs tend to be detected in those regions by SNP microarrays. Even if such CNVRs are false positives, our data set is still useful for screening large numbers of candidate CNVs.

It is unclear whether CNVs are selectively neutral on the basis of genetic drift, but they are certainly distributed throughout all human populations. Using the genotypes of mitochondrial DNA and Y chromosome, geneticists and anthropologists have surmised various intriguing scenarios about the history of humans.[37–40] However, these genetic materials have been transmitted exclusively through maternal and paternal lineages, respectively. In contrast, the CNVs reported here occur in the more extensive remaining genome regions; that is, on autosomes or the X chromosome. Therefore, they have acted some times as maternal alleles at and at other times as paternal alleles. They might also have been subjected to crossingover. CNV data from various parts of the world are essential to substantiate these hypothetical scenarios.

Chromosomal anomalies are found with conventional cytogenetic techniques in approximately half of all early sporadic miscarriages.[41] It is possible that miscarriages and pregnancy losses are also caused by submicroscopic chromosomal changes, including CNVs. Twenty-eight CNVs have been reported as candidate miscarriage-related variations when instances of recurrent pregnancy loss were examined by Rajcan-Separovic *et al.*[42] When 17 Caucasian and three African-American couples with recurrent pregnancy losses and their miscarriage samples were examined, CNVs that may have been related to miscarriages were reported.[42] They reported 11 novel CNVs in miscarriage samples and three in the parent samples and suggested that these CNVs were probably mutations causing susceptibility to miscarriage. Of the 11 CNVs in the miscarriage samples, one on chromosome 12 (130 060 706–130 430 847 in hg18) and another one on chromosome X (6 498 521–8 091 951) overlapped with our data set. Whereas the first one on chromosome 12 was up to 370 kb in length and encompassed the *GPR133* gene, the corresponding variable region in our data set is much shorter and includes no known genes. The *GPR133* gene encodes one of the orphan G-protein-coupled receptors, but its function is unknown.[43] It is possible that this receptor protein has a role in several signal-transduction pathways via classical receptor/G-protein interactions. Therefore, the CNV mentioned above may be a variant that causes miscarriage. However, one of the CNVs on chromosome X is consistent with our data set, suggesting that it is a commonly observed variant. In fact, Rajcan-Separovic *et al.*[42] tried to define the common CNVs using a collective repository in the DGV, but insufficient phenotypic information was available to refine the data. Taking these observations together, it seems that to define a set of common CNVs, it will be necessary to collect a large number of control data that focus on a specific phenotype; such as, normal parity in this case.

The Japanese are an admixture of ancient Asian populations that inhabited regions outside the Japanese Archipelago. We investigated the similarities among the CNVRs detected in various populations and noted that around 15% of Japanese CNVRs overlap those of other populations (Table 2). It has been suggested that the number of overlapping CNVs is influenced by the number of subjects. For instance, Japanese and Tibetan data showed dissimilarity because of the limited number of Tibetan subjects. Although the sample sizes of the Korean and Chinese populations are smaller than those of the European and African populations, similarities between the Japanese and other East Asian populations were similar to those of the European and African populations. This probably suggests strong similarities between the Japanese and other East Asian populations.

Previous studies have predominantly targeted European and African populations, but CNVs have been observed at different frequencies or copy numbers in different populations; for example, variations in the salivary amylase gene.[44] Many CNVs; such as, those at the *AMY1* locus, may be associated with diabetes, asthma, hypertension, allergy and other diseases of affluence in each ethnic group. Although CNVRs may result from the accumulation of tolerable structural mutations in the course of an ethnic history, they could start to influence the population's susceptibility to disease once its lifestyle is altered. The allelic frequencies of SNPs and short indels in each population have recently been documented.[45] The complete documentation of the CNVRs in each ethnic group is similarly important. The development of an innovative method to achieve this; such as, one involving next-generation sequencing and informatics, is another challenge.

CONFLICT OF INTEREST

The authors received no financial support from Illumina KK and the company had no role in the study design. The authors declare no conflict of interest.

ACKNOWLEDGEMENTS

We are grateful to all the participants in the present study, including the 411 women. Computation time was partly provided by the supercomputer system, Shirokane, at the Human Genome Centre, Institute of Medical Science, University of Tokyo. This work was supported by CREST Program 'Epigenomic analysis of the human placenta and endometrium constituting the fetal-maternal interface' of Japan Science and Technology Agency (JST) and Health and Labor Sciences Research Grants for Research into Rare and Intractable Diseases (H23 Jitsuyoka (Nanbyo)-Ippan-003 and H25 Jisedai-Ippan-001), and was also partly supported by KAKENHI 23770273, 24657151, 24390251, 24592494, 24659742, 25293345 and 25860258.

1 Redon, R., Ishikawa, S., Fitch, K. R., Feuk, L., Perry, G. H., Andrews, T. D. *et al.* Global variation in copy number in the human genome. *Nature* **444**, 444–454 (2006).
2 Stranger, B. E., Forrest, M. S., Dunning, M., Ingle, C. E., Beazley, C., Thorne, N. *et al.* Relative impact of nucleotide and copy number variation on gene expression phenotypes. *Science* **315**, 848–853 (2007).
3 Pang, A. W., Migita, O., Macdonald, J. R., Feuk, L. & Scherer, S. W. Mechanisms of formation of structural variation in a fully sequenced human genome. *Hum. Mut.* **34**, 345–354 (2013).
4 Frazer, K. A., Chen, X., Hinds, D. A., Pant, P. V., Patil, N. & Cox, D. R. Genomic DNA insertions and deletions occur frequently between humans and nonhuman primates. *Genome Res.* **13**, 341–346 (2003).
5 Locke, D. P., Segraves, R., Carbone, L., Archidiacono, N., Albertson, D. G., Pinkel, D. *et al.* Large-scale variation among human and great ape genomes determined by array comparative genomic hybridization. *Genome Res.* **13**, 347–357 (2003).
6 Sebat, J., Lakshmi, B., Troge, J., Alexander, J., Young, J., Lundin, P. *et al.* Large-scale copy number polymorphism in the human genome. *Science* **305**, 525–528 (2004).
7 Sharp, A. J., Locke, D. P., McGrath, S. D., Cheng, Z., Bailey, J. A., Vallente, R. U. *et al.* Segmental duplications and copy-number variation in the human genome. *Am. J. Hum. Genet.* **77**, 78–88 (2005).

8 Marshall, C. R. & Scherer, S. W. Detection and characterization of copy number variation in autism spectrum disorder. *Methods Mol. Biol.* **838**, 115–135 (2012).
9 Swaminathan, G. J., Bragin, E., Chatzimichali, E. A., Corpas, M., Bevan, A. P., Wright, C. F. *et al.* DECIPHER: web-based, community resource for clinical interpretation of rare variants in developmental disorders. *Hum. Mol. Genet.* **21**, R37–R44 (2012).
10 Firth, H. V., Richards, S. M., Bevan, A. P., Clayton, S., Corpas, M., Rajan, D. *et al.* DECIPHER: Database of Chromosomal Imbalance and Phenotype in Humans Using Ensembl Resources. *Am. J. Hum. Genet.* **84**, 524–533 (2009).
11 Macdonald, J. R., Ziman, R., Yuen, R. K., Feuk, L. & Scherer, S. W. The Database of Genomic Variants: a curated collection of structural variation in the human genome. *Nucleic Acids Res.* **42**, D986–D992 (2014).
12 Li, J., Yang, T., Wang, L., Yan, H., Zhang, Y., Guo, Y. *et al.* Whole genome distribution and ethnic differentiation of copy number variation in Caucasian and Asian populations. *PLoS ONE* **4**, e7958 (2009).
13 Lou, H., Li, S., Yang, Y., Kang, L., Zhang, X., Jin, W. *et al.* A map of copy number variations in Chinese populations. *PLoS ONE* **6**, e27341 (2011).
14 Zhang, Y. B., Li, X., Zhang, F., Wang, D. M. & Yu, J. A preliminary study of copy number variation in Tibetans. *PLoS ONE* **7**, e41768 (2012).
15 Kanduri, C., Ukkola-Vuoti, L., Oikkonen, J., Buck, G., Blancher, C., Raijas, P. *et al.* The genome-wide landscape of copy number variations in the MUSGEN study provides evidence for a founder effect in the isolated Finnish population. *Eur. J. Hum. Genet.* **21**, 1411–1516 (2013).
16 Hanihara, K. Dual structure model for the population history of the Japanese. *Jpn Rev.* **2**, 1–33 (1991).
17 Japanese Archipelago Human Population Genetics C., Jinam, T., Nishida, N., Hirai, M., Kawamura, S., Oota, H. *et al.* The history of human populations in the Japanese Archipelago inferred from genome-wide SNP data with a special reference to the Ainu and the Ryukyuan populations. *J. Hum. Genet.* **57**, 787–795 (2012).
18 Wang, K., Li, M., Hadley, D., Liu, R., Glessner, J., Grant, S. F. *et al.* PennCNV: an integrated hidden Markov model designed for high-resolution copy number variation detection in whole-genome SNP genotyping data. *Genome Res.* **17**, 1665–1674 (2007).
19 Pritchard, J. K., Stephens, M. & Donnelly, P. Inference of population structure using multilocus genotype data. *Genetics* **155**, 945–959 (2000).
20 Kumasaka, N., Yamaguchi-Kabata, Y., Takahashi, A., Kubo, M., Nakamura, Y. & Kamatani, N. Establishment of a standardized system to perform population structure analyses with limited sample size or with different sets of SNP genotypes. *J. Hum. Genet.* **55**, 525–533 (2010).
21 McCarroll, S. A., Kuruvilla, F. G., Korn, J. M., Cawley, S., Nemesh, J., Wysoker, A. *et al.* Integrated detection and population-genetic analysis of SNPs and copy number variation. *Nat. Genet.* **40**, 1166–1174 (2008).
22 Conrad, D. F., Pinto, D., Redon, R., Feuk, L., Gokcumen, O., Zhang, Y. *et al.* Origins and functional impact of copy number variation in the human genome. *Nature* **464**, 704–712 (2010).
23 Koike, A., Nishida, N., Yamashita, D. & Tokunaga, K. Comparative analysis of copy number variation detection methods and database construction. *BMC Genet.* **12**, 29 (2011).
24 Moon, S., Kim, Y. J., Hong, C. B., Kim, D. J., Lee, J. Y. & Kim, B. J. Data-driven approach to detect common copy-number variations and frequency profiles in a population-based Korean cohort. *Eur. J. Hum. Genet.* **19**, 1167–1172 (2011).
25 Vogler, C., Gschwind, L., Rothlisberger, B., Huber, A., Filges, I., Miny, P. *et al.* Microarray-based maps of copy-number variant regions in European and sub-Saharan populations. *PLoS ONE* **5**, e15246 (2010).
26 Shaikh, T. H., Gai, X., Perin, J. C., Glessner, J. T., Xie, H., Murphy, K. *et al.* High-resolution mapping and analysis of copy number variations in the human genome: a data resource for clinical and research applications. *Genome Res.* **19**, 1682–1690 (2009).
27 Fanciulli, M., Norsworthy, P. J., Petretto, E., Dong, R., Harper, L., Kamesh, L. *et al.* FCGR3B copy number variation is associated with susceptibility to systemic, but not organ-specific, autoimmunity. *Nat. Genet.* **39**, 721–723 (2007).
28 Willcocks, L. C., Lyons, P. A., Clatworthy, M. R., Robinson, J. I., Yang, W., Newland, S. A. *et al.* Copy number of FCGR3B, which is associated with systemic lupus erythematosus, correlates with protein expression and immune complex uptake. *J. Exp. Med.* **205**, 1573–1582 (2008).
29 McKinney, C. & Merriman, T. R. Meta-analysis confirms a role for deletion in FCGR3B in autoimmune phenotypes. *Hum. Mol. Genet.* **21**, 2370–2376 (2012).
30 Yang, T. L., Chen, X. D., Guo, Y., Lei, S. F., Wang, J. T., Zhou, Q. *et al.* Genome-wide copy-number-variation study identified a susceptibility gene, UGT2B17, for osteoporosis. *Am. J. Hum. Genet.* **83**, 663–674 (2008).
31 Jakobsson, J., Ekström, L., Inotsume, N., Garle, M., Lorentzon, M., Ohlsson, C. *et al.* Large differences in testosterone excretion in Korean and Swedish men are strongly associated with a UDP-glucuronosyl transferase 2B17 polymorphism. *J. Clin. Endocrinol. Metab.* **91**, 687–693 (2006).
32 Pianezza, M. L., Sellers, E. M. & Tyndale, R. F. Nicotine metabolism defect reduces smoking. *Nature* **393**, 750 (1998).
33 Miyamoto, M., Umetsu, Y., Dosaka-Akita, H., Sawamura, Y., Yokota, J., Kunitoh, H. *et al.* CYP2A6 gene deletion reduces susceptibility to lung cancer. *Biochem. Biophys. Res. Commun.* **261**, 658–660 (1999).
34 Lv, J., Yang, Y., Zhou, X., Yu, L., Li, R., Hou, P. *et al.* FCGR3B copy number variation is not associated with lupus nephritis in a Chinese population. *Lupus* **19**, 158–161 (2010).
35 Xue, Y., Sun, D., Daly, A., Yang, F., Zhou, X., Zhao, M. *et al.* Adaptive evolution of UGT2B17 copy-number variation. *Am. J. Hum. Genet.* **83**, 337–346 (2008).
36 Oscarsona, M., McLellana, R. A., Gullstenb, H., Yuec, Q. Y., Langd, M. A., Bernale, M. L. *et al.* Characterisation and PCR-based detection of a CYP2A6 gene deletion found at a high frequency in a Chinese population. *FEBS Lett.* **448**, 105–110 (1999).
37 Hammer, M. F. & Horai, S. Y chromosomal DNA variation and the peopling of Japan. *Am. J. Hum. Genet.* **56**, 951–962 (1995).
38 Shinka, T., Tomita, K., Toda, T., Kotlarova, S. E., Lee, J., Kuroki, Y. *et al.* Genetic variations on the Y chromosome in the Japanese population and implications for modern human Y chromosome lineage. *J. Hum. Genet.* **44**, 240–245 (1999).
39 Dulik, M. C., Zhadanov, S. I., Osipova, L. P., Askapuli, A., Gau, L., Gokcumen, O. *et al.* Mitochondrial DNA and Y chromosome variation provides evidence for a recent common ancestry between Native Americans and Indigenous Altaians. *Am. J. Hum. Genet.* **90**, 229–246 (2012).
40 Oppenheimer, S. Out-of-Africa, the peopling of continents and islands: tracing uniparental gene trees across the map. *Philos. Trans. R. Soc. Lond. Ser. B* **367**, 770–784 (2012).
41 van den Berg, M., van Maarle, M., van Wely, M. & Goddijn, M. Genetics of early miscarriage. *Biochim. Biophys. Acta* **1822**, 1951–1959 (2012).
42 Rajcan-Separovic, E., Diego-Alvarez, D., Robinson, W. P., Tyson, C., Qiao, Y., Harvard, C. *et al.* Identification of copy number variants in miscarriages from couples with idiopathic recurrent pregnancy loss. *Hum. Reprod.* **25**, 2913–2922 (2010).
43 Bohnekamp, J. & Schoneberg, T. Cell adhesion receptor GPR133 couples to Gs protein. *J. Biol. Chem.* **286**, 41912–41916 (2011).
44 Perry, G. H., Dominy, N. J., Claw, K. G., Lee, A. S., Fiegler, H., Redon, R. *et al.* Diet and the evolution of human amylase gene copy number variation. *Nat. Genet.* **39**, 1256–1260 (2007).
45 1000 Genomes Project Consortium, Abecasis, G. R., Auton, A., Brooks, L. D., DePristo, M. A., Durbin, R. M. *et al.* An integrated map of genetic variation from 1092 human genomes. *Nature* **491**, 56–65 (2012).

Supplementary Information accompanies the paper on Journal of Human Genetics website (http://www.nature.com/jhg)

Pediatr Nephrol
DOI 10.1007/s00467-014-3007-0

BRIEF REPORT

Renal function in angiotensinogen gene-mutated renal tubular dysgenesis with glomerular cysts

Satoshi Hibino · Hiroshi Sasaki · Yoshifusa Abe · Akira Hojo · Mitsugu Uematsu · Takashi Sekine · Kazuo Itabashi

Received: 27 September 2014 / Revised: 28 October 2014 / Accepted: 5 November 2014

Abstract
Background Inherited renal tubular dysgenesis (RTD) is caused by mutations in the genes encoding the components of the renin–angiotensin system (RAS). RTD is characterized by oligohydramnios, renal failure, neonatal hypocalvaria, and severe hypotension. The histological characteristics, underlying mechanism, and long-term prognosis remain poorly known.
Case-diagnosis/treatment We describe here a 4-year-old female with RTD. Endocrinologic analysis showed a discrepancy between low plasma renin activity and high active renin concentration, suggesting a loss of the renin substrate, angiotensinogen (AGT). Direct sequencing revealed a frameshift deletion at nucleotide 1,355 in exon 5 in the AGT gene. Although a histological hallmark is regarded to be the absence or poor development of the proximal tubule, the patient does have minimally impaired function of the proximal tubule. Glomerular cysts without glomerular tufts were noted in approximately half of the glomeruli. The urinary concentrating ability and sodium reabsorption and potassium excretion in the distal nephron were severely affected.
Conclusions The patient has an impaired function of the distal nephron despite minimally affected function of the proximal tubule, probably attributed to renal tubular dysgenesis and fetal hypoperfusion. The renal tubular maturity and the severity of ischemic injury may be key determinants of the clinical symptoms and pathological findings in RTD, in which the RAS plays an important role.

Keywords Renal tubular dysgenesis · Angiotensinogen · Rennin–angiotensin system · Nephrogenic diabetes insipidus · Glomerular cysts

S. Hibino (✉) · H. Sasaki · Y. Abe · A. Hojo · K. Itabashi
Department of Pediatrics, Showa University School of Medicine, 1-5-8 Hatanodai, Shinagawa-ku, Tokyo 142-8666, Japan
e-mail: satohibino@yahoo.co.jp

M. Uematsu
Department of Pediatrics, Tohoku University Graduate School of Medicine, Miyagi, Japan

T. Sekine
Department of Pediatrics, Ohashi Medical Center, Toho University, Tokyo, Japan

Published online: 22 November 2014

Introduction

Renal tubular dysgenesis (RTD) is clinically characterized by oligohydramnios, anuria, hypoplastic lung, hypocalvaria, and severe hypotension, as well as by the absence or poor development of the proximal tubule [1]. Inherited RTD is caused by mutations in the genes encoding the components of the renin–angiotensin system (RAS) [2]. Mutations in the genes encoding angiotensinogen (AGT), renin, angiotensin-converting enzyme (ACE), and angiotensin II receptor type 1 have been reported in several case reports [1, 3–8]. RTD is also associated with fetopathy induced by drugs such as angiotensin-converting enzyme inhibitors (ACEIs) or angiotensin type 1 receptor blockers (ARBs) [9–11]. Despite several case reports of patient survival [3–8], the long-term renal prognosis remains poorly known. Here we report our evaluation of the physiologic and histopathological characteristics of the kidneys and renal tubules in a 4-year-old girl with RTD caused by a mutation in the *AGT* gene.

Case report

The patient was a 4-year-old Japanese girl, the first child of healthy non-consanguineous parents. The mother was not given ACEIs or ARBs during her pregnancy. The infant was delivered by emergency cesarean section at 32 weeks immediately after detection of oligohydramnios and subsequent fetal distress. She had a body weight of 1,669 g and had hypoplastic lung and hypocalvaria. After birth, she received mechanical ventilation and nitric oxide inhalation therapy for pneumothorax and persistent pulmonary hypertension. She had severe systemic hypotension episodes (mean blood pressure 20–25 mmHg), and a slight improvement in blood pressure was achieved by the intravenous infusion of fresh frozen plasma and catecholamines. The patient required peritoneal dialysis due to anuria on days 3–13 after birth. Her serum potassium and creatinine concentrations peaked at 7.2 mEq/L and 2.8 mg/dL, respectively. Spontaneous urination was first observed on day 10.

After the infant had recovered from these conditions, polyuria, hyponatremia, and hyperkalemia occurred. Her serum creatinine concentration rapidly decreased to 0.4 mg/dL by day 35, during which time her blood pressure remained within normal range without any medication. Endocrinologic analysis showed a discrepancy between low plasma renin activity (<0.1 ng/mL/h) and high active renin concentration (11,400 pg/mL), suggesting an abnormality or loss of the renin substrate, AGT. These conditions were strongly suggestive of RTD. Informed consent for gene analysis was obtained from her parents, and direct sequencing revealed a frameshift deletion at nucleotide 1,355 in exon 5 in the coding region of the *AGT* gene (c.1355delT, p.Leu452CysfsX2). Gene analysis of her parents was not performed.

At the age of 2 years and 4 months, she occasionally required hospitalization due to hypotonic dehydration. At this time, her height was 83.5 cm [−1.0 standard deviation (SD)] and her weight was 9.7 kg (−1.9 SD). Her creatinine clearance rate (CCr) had decreased to 72–88 mL/min/1.73 m^2. Due to polyuria (150–200 mL/kg/day), high fluid intake was required. A water deprivation test showed a maximum urine osmolality of 183 mOsm/kg, without any response to injected arginine vasopressin. The condition indicated nephrogenic diabetes insipidus (NDI). Her fractional excretion of sodium (FENa) was 1.0–3.7 % and her estimated glomerular filtration rate was not markedly decreased, suggesting that her condition was a result of impaired sodium reabsorption. At this time, her fractional excretion of potassium (FEK) was 2.0–3.5 % (normal range 11.2±5.4 %), and her transtubular potassium concentration gradient (TTKG) was 1.2 (normal range >5). Consequently, she required sodium supplementation (7–9 mEq/kg/day) and restricted potassium intake (0.6 mEq/kg/day). Blood gas analysis showed mild acidosis. Her urinary beta2-microglobulin (beta2-MG) concentration, fractional excretion of uric acid (FEUA), and transtubular reabsorption rate of phosphate (%TRP) fell almost within normal ranges. Glucosuria, proteinuria, and aminoaciduria were not detected. These results indicated that her proximal tubular cells functioned normally, but that urinary concentrating ability and potassium excretion in the distal nephron were severely affected. Endocrine laboratory data were as follows: angiotensin I, 340 pg/mL (normal range <500 pg/mL); an angiotensin II 13 pg/mL (normal range 9–47 pg/mL); aldosterone 98 pg/dL (normal range 36–240 pg/dL); ACE 21.3 IU/L (normal range 8.3–21.4 IU/L); urinary cyclic AMP 6×10^{-6} μmol/day (normal range 2–7 μmol/day).

A renal biopsy was performed at the age of 2 years and 5 months. Light microscopy examination, which enabled the specific identification of the cortex and the medulla, revealed that of the 80 glomeruli examined, 12 (15 %) were normal, eight (10 %) were sclerotic, eight (10 %) were fetal type, and 52 (65 %) had dilated Bowman's capsules, approximately half of which had glomerular cysts without glomerular tufts (Fig. 1a). Renal tubular atrophy and interstitial fibrosis were observed in the cortex. Surviving proximal tubules in the cortex were positive for CD10 (a 100-kDa cell-surface zinc metalloendopeptidase) (Fig. 1b) [12]. Epithelial membrane antigen staining showed that the distal tubules and collecting ducts were present in the cortex and medulla (Fig. 1c), and Henle loops stained positive for Tamm–Horsfall protein (THP) in the medulla (Fig. 1d). Also, a large number of cells in the juxglomerular apparatus were strongly positive for anti-renin antibody (Fig. 1e). The muscular wall in the interlobular and preglomerular arteries was thickened and positive for alpha-smooth muscle actin (Fig. 1f).

Discussion

We describe here a 4-year-old girl diagnosed with RTD who survived. A definitive diagnosis of RTD was made on the basis of clinical manifestations, high plasma renin concentration, low renin activity, and sequencing of *AGT*. Pathological findings, including the overproduction of renin and thickening of the muscular wall in the arteries, were consistent with prior case reports of RTD [1, 3, 5–7]. Although a histological hallmark is regarded as the absence or poor development of the proximal tubule [1], our patient has almost normal components of the proximal tubule. In addition, glomerular cysts, which are uncommon in RTD patients, were noted. The results of functional analyses are consistent with the pathological findings.

To our knowledge, nine surviving RTD patients with inherited mutation-induced RAS inactivity have been reported in the literature. Of these nine patients, two had *AGT* mutations, six had *ACE* mutations, and one had a *REN* mutation [3–8]. Regarding the two patients with *AGT* mutations, a pair of siblings had a homozygous missense mutation [4], and on patient had a heterozygous mutation [3]. Despite these patients having the mutations in a same component of the RAS gene, their clinical and histological findings were not consistent. The long-term renal prognosis and tubular function of RTD patients remain poorly known. Our report on the

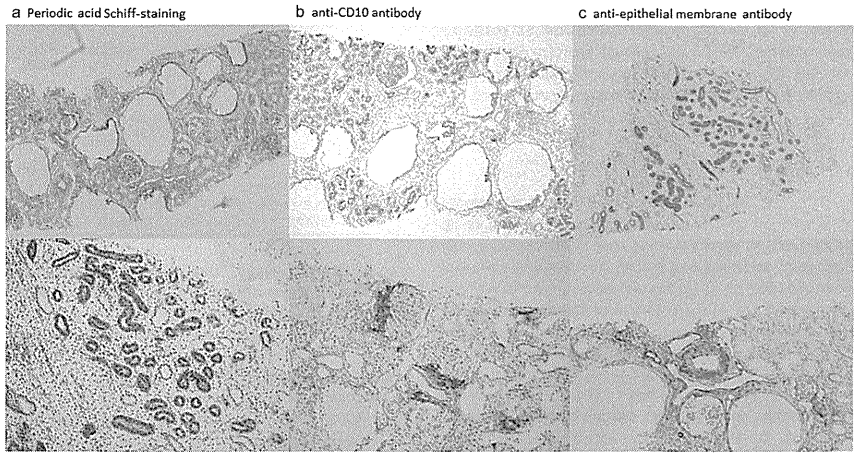

Fig. 1 Renal biopsy findings in our patient. **a** Several dilated Bowman's capsules lacked the glomerular tuft. Renal tubular atrophy and interstitial fibrosis were observed in the cortex. Periodic acid-Schiff staining (original magnification ×100). **b** Presence in the cortex of several remnant proximal tubules immunolabeled with anti-CD10 antibody which recognizes the human-membrane-associated neutral endopeptidase of podocytes and proximal tubular cells (original magnification ×100). **c** Distal tubules and collecting ducts in the medulla labeled with antibody to epithelial membrane antigen (original magnification ×100). **d** Presence in the medulla of Henle loops labeled with Tamm–Horsfall protein (original magnification ×400). **e** High renin production in the enlarged juxtaglomerular apparatus (original magnification ×400). **f** Thickening of the muscular walls in the interlobular and preglomerular arteries labeled with antibody to alpha-smooth muscle actin (original magnification ×400)

morphological and functional effects of the RAS on the developing kidney of children with RTD caused by mutations in the AGT gene is therefore note-worthy.

The morphological and functional abnormalities in the kidney of RTD patients are likely associated with two factors: abnormal nephrogenesis due to mutation-induced RAS inactivity and ischemic injury due to fetal or neonatal hypoperfusion. Although the main histopathological hallmark of RTD has been reported to be impairment of the proximal tubules [1], recent case reports have described non-specific pathological findings in patients with similar mutations. In a patient with a *REN* mutation who underwent renal transplantation [4], the proximal tubules were positive for CD15 (cluster of differentiation antigen) in the nephrectomy specimen at the age of 9 years, but were negative on day 9 after birth [4]. This observation suggested that the proximal tubule continued to mature or had recovered from ischemic injury. In our patient, the amount of amniotic fluid indicated she had the ability to produce urine during the fetal period. Her sudden urination at age 10 days suggests a successful recovery from acute tubular necrosis associated with fetal hypoperfusion and ischemic injury. Pathological findings in patients with RTD, especially in surviving patients, may vary depending on the severity of renal dysgenesis and ischemic injury.

Extremely dilated Bowman's capsules, i.e., glomerular cysts without glomerular tufts, were noted in our patient. The absence of glomerular tufts suggests that some glomerular tufts should be affected by urine flooding associated with disconnections in distal nephrons. These were considered to be the result of renal dysgenesis and ischemic damage. A decreased number of nephrons may be associated with hyperfiltration and dilation of Bowman's capsules. These pathological findings may be affected by the timing of the renal biopsy as glomerular cysts are possibly detectable only several years after birth in surviving patients.

The CCr of our patient was only mildly decreased, probably due to the survival of some of the glomeruli. The almost normal urinary levels of beta$_2$-MG, FEUA, and %TRP indicate that the proximal tubules of our patient were minimally affected. These findings are consistent with the pathological results, including coexistence of partly normal remnant proximal and distal tubules with renal tubular atrophy and fibrosis in interstitial tissue. The water deprivation test and FENa, FEK, and TTKG values showed that she had NDI with

dysfunction of sodium reabsorption and potassium excretion, as reported previously in a patient with ARB fetopathy [9]. Hence, her conditions were probably caused by functional and structural immaturity of the distal tubules and collecting ducts create the osmotic gradient by controlling sodium and potassium balance in the medulla. These disorders may lead to the abnormal expression of the Na^+–K^+ transporters, the vasopressin receptor, and aquaporin and to an insufficient osmotic gradient, as well as to negative effects of aldosterone on cortical collecting ducts. Interestingly, several gene target mouse models, such as *AGT* and *AT1* receptor knock-out mice, have shown a markedly atrophic papilla and dilated pelvis due to polyuria [13, 14]. Rat models of ACEI and ARB fetopathy present with papillary atrophy, tubulointerstitial fibrosis, and tubular atrophy and dilation, resulting in impairment of their urinary concentrating ability [15, 16]. Renal tubular dysfunction and salt-losing NDI in our patient were compatible with the papillary atrophy observed in animal models. Although few morphological data on the medulla are available, we found that disorders of the RAS system in the human fetus may result in functional and morphological abnormalities of Henle's loop and the collecting ducts in the medulla associated with loss of inability to control salt and water balance.

In conclusion, the renal tubular dysfunction in our patient was characterized by NDI associated with sodium reabsorption and potassium excretion dysfunction in the medulla. RAS plays an important role on the main dysfunctional site in the distal nephrons. The key determinants of the outcomes of RTD may be renal tubular maturity and severity of ischemic injury after fetal and neonatal hypoperfusion.

Acknowledgments We wish to thank Dr. Osamu Uemura, Dr. Shuichiro Watanabe and Dr. Yutaka Yamaguchi for the clinical and pathological diagnosis of our patient. We also thank Dr. Jeffrey B. Kopp for his critical review of the manuscript.

Conflict of interest None.

References

1. Gubler MC, Antignac C (2010) Renin-angiotensin system in kidney development: renal tubular dysgenesis. Kidney Int 77:400–406
2. Gribouval O, Gonzales M, Neuhaus T, Aziza J, Bieth E, Laurent N, Bouton JM, Feuillet F, Makni S, Ben Amar H, Laube G, Delezoide AL, Bouvier R, Dijoud F, Ollagnon-Roman E, Roume J, Joubert M, Antignac C, Gubler MC (2005) Mutations in genes in the renin-angiotensin system are associated with autosomal recessive renal tubular dysgenesis. Nat Genet 37:964–968
3. Uematsu M, Sakamoto O, Nishio T, Ohura T, Matsuda T, Inagaki T, Abe T, Okamura K, Kondo Y, Tsuchiya S (2006) A case surviving for over a year of renal tubular dysgenesis with compound heterozygous angiotensinogen gene mutations. Am J Med Genet A 140:2355–2360
4. Zingg-Schenk A, Bacchetta J, Corvol P, Michaud A, Stallmach T, Cochat P, Gribouval O, Gubler MC, Neuhaus TJ (2008) Inherited renal tubular dysgenesis: the first patients surviving the neonatal period. Eur J Pediatr 167:311–316
5. Uematsu M, Sakamoto O, Ohura T, Shimizu N, Satomura K, Tsuchiya S (2009) A further case of renal tubular dysgenesis surviving the neonatal period. Eur J Pediatr 168:207–209
6. Schreiber R, Gubler MC, Gribouval O, Shalev H, Landau D (2010) Inherited renal tubular dysgenesis may not be universally fatal. Pediatr Nephrol 25:2531–2534
7. Gribouval O, Moriniere V, Pawtowski A, Arrondel C, Sallinen SL, Saloranta C, Clericuzio C, Viot G, Tantau J, Blesson S, Cloarec S, Machet MC, Chitayat D, Thauvin C, Laurent N, Sampson JR, Bernstein JA, Clemenson A, Prieur F, Daniel L, Levy-Mozziconacci A, Lachlan K, Alessandri JL, Cartault F, Riviere JP, Picard N, Baumann C, Delezoide AL, Belar Ortega M, Chassaing N, Labrune P, Yu S, Firth H, Wellesley D, Bitzan M, Alfares A, Braverman N, Krogh L, Tolmie J, Gaspar H, Doray B, Majore S, Bonneau D, Triau S, Loirat C, David A, Bartholdi D, Peleg A, Brackman D, Stone R, DeBerardinis R, Corvol P, Michaud A, Antignac C, Gubler MC (2012) Spectrum of mutations in the renin-angiotensin system genes in autosomal recessive renal tubular dysgenesis. Hum Mutat 33:316–326
8. Danilov SM, Kalinin S, Chen Z, Vinokour EI, Nesterovitch AB, Schwartz DE, Gribouval O, Gubler MC, Minshall RD (2010) Angiotensin I-converting enzyme Gln1069Arg mutation impairs trafficking to the cell surface resulting in selective denaturation of the C-domain. PLoS ONE 5:e10438
9. Miura K, Sekine T, Iida A, Takahashi K, Igarashi T (2009) Salt-losing nephrogenic diabetes insipidus caused by fetal exposure to angiotensin receptor blocker. Pediatr Nephrol 24:1235–1238
10. Laube GF, Kemper MJ, Schubiger G, Neuhaus TJ (2007) Angiotensin-converting enzyme inhibitor fetopathy: long-term outcome. Arch Dis Child Fetal Neonatal Ed 92:F402–F403
11. Quan A (2006) Fetopathy associated with exposure to angiotensin converting enzyme inhibitors and angiotensin receptor antagonists. Early Hum Dev 82:23–28
12. Martigoni G, Pea M, Brunelli M, Chilosi M, Zamó A, Bertaso M, Cossu-Rocca P, Eble JN, Mikuz G, Puppa G, Badoual C, Ficarra V, Novella G, Bonetti F (2004) CD10 is expressed in a subset of chromophobe renal cell carcinomas. Mod Pathol 17:1455–1463
13. Kihara M, Umemura S, Sumida Y, Yokoyama N, Yabana M, Nyui N, Tamura K, Murakami K, Fukamizu A, Ishii M (1998) Genetic deficiency of angiotensinogen produces an impaired urine concentrating ability in mice. Kidney Int 53:548–555
14. Tsuchida S, Matsusaka T, Chen X, Okubo S, Niimura F, Nishimura H, Fogo A, Utsunomiya H, Inagami T, Ichikawa I (1998) Murine double nullizygotes of the angiotensin type 1A and 1B receptor genes duplicate severe abnormal phenotypes of angiotensinogen nullizygotes. J Clin Invest 101:755–760
15. Guron G, Nilsson A, Nitescu N, Nielsen S, Sundelin B, Frokiaer J, Friberg P (1999) Mechanisms of impaired urinary concentrating ability in adult rats treated neonatally with enalapril. Acta Physiol Scand 165:103–112
16. Chen Y, Lasaitiene D, Gabrielsson BG, Carlsson LM, Billig H, Carlsson B, Marcussen N, Sun XF, Friberg P (2004) Neonatal losartan treatment suppresses renal expression of molecules involved in cell-cell and cell-matrix interactions. J Am Soc Nephrol 15:1232–1243

Images in CAD

Coronary Artery Disease 2014, 25:727–729

Five-year follow-up of a giant coronary aneurysm using virtual coronary angioscopy

Yasushi Akutsu[a,b], Youichi Kobayashi[b], Takehiko Sambe[a,c], Toshikazu Kurihara[a], Kyouichi Kaneko[b], Yusuke Kodama[b], Hui-Ling Li[b], Jumpei Suyama[d], Yuji Hamazaki[b], Junya Iwasaki[c], Takehiko Gokan[d], Kazuo Itabashi[c], Katsuji Oguchi[e], Naoki Uchida[a,c] and Shinichi Kobayashi[a], [a]Department of Internal Medicine (Cardiology), Clinical Research Institute for Clinical Pharmacology & Therapeutics, Showa University Karasuyama Hospital, [b]Department of Medicine, Division of Cardiology, Departments of [c]Pediatrics, [d]Radiology and [e]Pharmacology, Showa University School of Medicine, Tokyo, Japan

Correspondence to Yasushi Akutsu, MD, PhD, Department of Internal Medicine (Cardiology), Clinical Research Institute for Clinical Pharmacology & Therapeutics, Showa University Karasuyama Hospital, 6-11-11 Kita-Karasuyama, Setagayaku, Tokyo 157-8577, Japan
Tel: +81 3 3300 5247; fax: +81 3 3300 1653;
e-mail: hzn01233@s02.itscom.net

Received 30 May 2014 Revised 28 June 2014 Accepted 2 July 2014

An 8-year-old male was diagnosed with Kawasaki disease (KD) with a giant coronary aneurysm in the origin of the left anterior descending artery on echocardiography. When he was 15, 17, and 20 years old, 128-slice multidetector computed tomography (MDCT) (Somatom Definition AS+; Siemens Healthcare, Forchheim, Germany) was performed. The sectional view of the coronary artery on MDCT showed a persistent aneurysmal diameter of 8 mm with gradually progressing calcification and a persistent plaque in the aneurysm over a period of 5 years (Fig. 1a). The virtual coronary angioscopy (VCA) was constructed along the left anterior descending artery from the MDCT data using the 'SYNAPSE VINCENT' three-dimensional volume analyzer software (Fujifilm Co., Tokyo, Japan), indicating the remarkable progression of the coronary artery stenosis caused by calcifications at both edges of the coronary aneurysm (Fig. 1a). The coronary angiography (CAG) was performed at 11, 17, and 20 years of age and detected persistent 75% stenosis on the proximal side of the coronary aneurysm at 17 and 20 years of age (Fig. 2). The fractional flow reserve (FFR) using a pressure wire was measured invasively during the CAG at 20 years of age and indicated 0.75 on the distal side of the site of coronary artery stenosis. The optical coherence tomography confirmed the coronary artery luminal narrowing with intimal thickening, the calcifications at both edges of the coronary aneurysm, and the plaques in the coronary aneurysm, similar to the VCA findings (Fig. 1b). Percutaneous transluminal coronary rotational atherectomy was performed repeatedly with burr sizes of 1.75 and 2.25 mm on the proximal edge of the coronary aneurysm (Fig. 2). As a result, the FFR in the stenotic lesion recovered to 0.93.

Coronary aneurysm formation and subsequent coronary artery stenosis resulting in ischemic heart disease and sudden death are the most important complications of KD [1]. Calcification is frequently observed in the area of coronary stenosis more than 6 years after onset. Therefore, a detailed evaluation of the severity and the extent of calcification is very important for optimal selection of suitable therapeutic procedures. Although intravascular ultrasound imaging or optical coherence tomography allows a detailed structural observation of the coronary artery wall, it is difficult in KD patients without symptoms to follow up the inner surface of the calcified coronary artery regularly using an invasive method. The conventional contrast-enhanced axial slices on MDCT are superior to VCA for lesion detection, particularly as noncalcified coronary lesions can be visualized with good diagnostic accuracy. However, VCA was found to be accurate in detecting complex lesions with an irregular surface and calcification because of the high density of the calcium deposits within the lumen. Compared with the conventional two-dimensional computed tomographic images, VCA can access the three-dimensional shape of irregularly calcificated surface on the inside of the lumen more precisely, although VCA may have tended to be visualized the coronary artery stenosis more urgently than the conventional MDCT [2]. However, the high computed tomographic density with the heavy calcifications that cover the entire lumen would make the stenosis of coronary artery vague because of a viewpoint from outside the coronary artery on the conventional MDCT findings. In fact, we confirmed the lower coronary flow with FFR than those on CAG and conventional MDCT findings. The success of percutaneous transluminal coronary rotational atherectomy is associated with a more demanding technique [3]. In conclusion, VCA may be useful not only for detecting the three-dimensional progression of the calcifications in a noninvasive manner but also aiding the choice of the subsequent intervention strategy.

Supplemental digital content is available for this article. Direct URL citations appear in the printed text and are provided in the HTML and PDF versions of this article on the journal's website (*www.coronary-artery.com*).

0954-6928 © 2014 Wolters Kluwer Health | Lippincott Williams & Wilkins

DOI: 10.1097/MCA.0000000000000157

Fig. 1

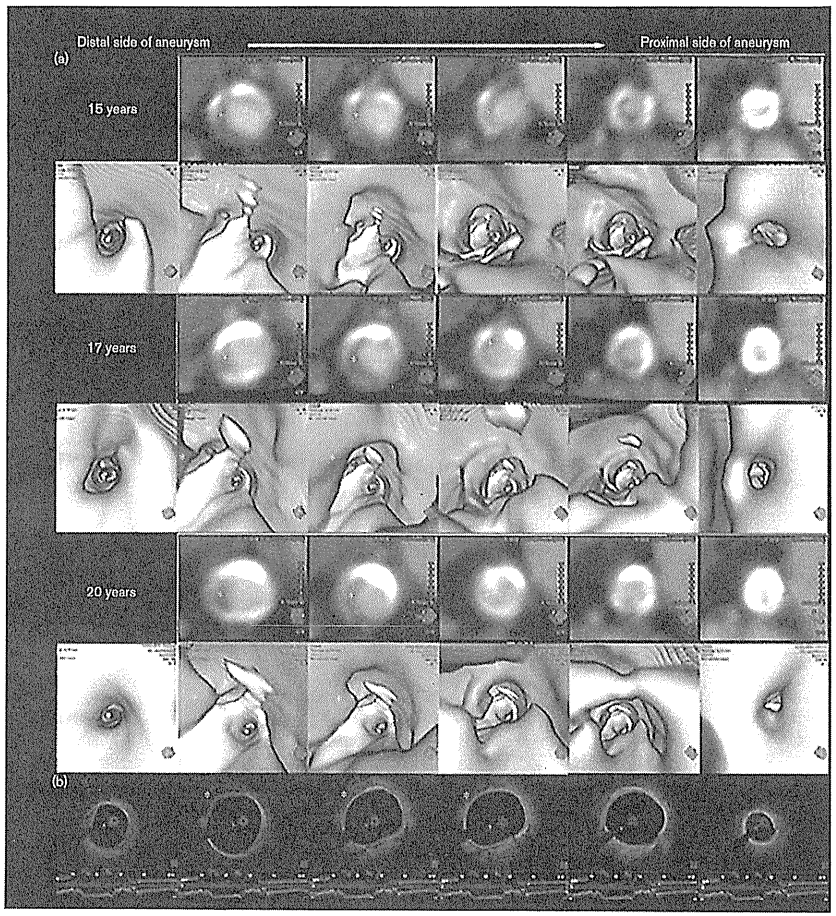

Sectional view of the coronary artery and virtual coronary angioscopic (VCA) view on multi-detector computed tomography imaging (a) (Supplemental Video I, Supplemental digital content 1, *http://links.lww.com/MCA/A16*) and optical coherence tomography (b) (Supplemental Video II, Supplemental digital content 2, *http://links.lww.com/MCA/A17*). The VCA was constructed by eliminating the lumen filled with contrast media, which was defined as having a computed tomographic (CT) density of 150–500 HU, and the calcification area greater than 500 HU was presented as a white color (450–500: the gradation). The vessel wall was defined as having a CT density of 150–200 HU, and was presented as a flesh color. Furthermore, the plaque was defined as having a CT density of greater than 150 HU, and was presented as a black color, and the wall side gradated the color for the CT density from 200 to 150 HU. *Plaque.

Fig. 2

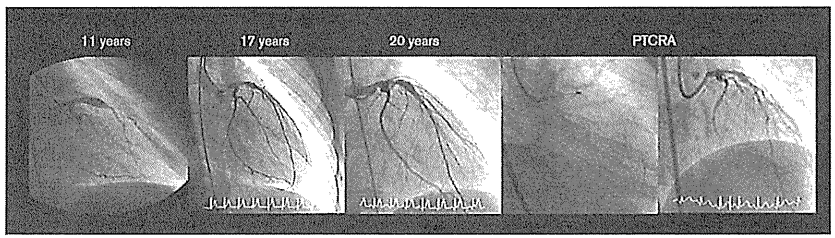

Coronary angiographic findings at 11, 17, and 20 years of age and PTCRA. The PTCRA was performed successfully at the proximal edge of the coronary aneurysm in the origin of left anterior descending artery. PTCRA, percutaneous transluminal coronary rotational atherectomy.

Acknowledgements

Conflicts of interest

There are no conflicts of interest.

References

1 Suda K, Iemura M, Nishiono H, Teramachi Y, Koteda Y, Kishimoto S, *et al.* Long-term prognosis of patients with Kawasaki disease complicated by giant coronary aneurysms: a single-institution experience. *Circulation* 2011; 123:1836–1842.

2 Schroeder S, Kopp AF, Ohnesorge B, Loke-Gie H, Kuettner A, Baumbach A, *et al.* Virtual coronary angioscopy using multislice computed tomography. *Heart* 2002; 87:205–209.

3 Akagi T. Interventions in Kawasaki disease. *Pediatr Cardiol* 2005; 26:206–212.

Early Human Development xxx (2014) xxx–xxx

Contents lists available at ScienceDirect

Early Human Development

journal homepage: www.elsevier.com/locate/earlhumdev

Accumulation of subcutaneous fat, but not visceral fat, is a predictor of adiponectin levels in preterm infants at term-equivalent age

Yuya Nakano *, Kazuo Itabashi, Motoichiro Sakurai, Madoka Aizawa, Kazushige Dobashi, Katsumi Mizuno

Department of Pediatrics, Showa University School of Medicine, Tokyo, Japan

ARTICLE INFO

Article history:
Received 15 October 2013
Received in revised form 19 February 2014
Accepted 24 February 2014
Available online xxxx

Keywords:
Adiponectin
Preterm infants
Subcutaneous fat
Visceral fat
Postnatal growth

ABSTRACT

Background: Preterm infants have altered fat tissue development, including a higher percentage of fat mass and increased volume of visceral fat. They also have altered adiponectin levels, including a lower ratio of high-molecular-weight adiponectin (HMW-Ad) to total adiponectin (T-Ad) at term-equivalent age, compared with term infants.
Aims: The objective of this study was to investigate the association between adiponectin levels and fat tissue accumulation or distribution in preterm infants at term-equivalent age.
Study design: Cross-sectional clinical study.
Subjects: Study subjects were 53 preterm infants born at ≤34 weeks gestation with a mean birth weight of 1592 g.
Outcome measures: Serum levels of T-Ad and HMW-Ad were measured and a computed tomography (CT) scan was performed at the level of the umbilicus at term-equivalent age to analyze how fat tissue accumulation or distribution was correlated with adiponectin levels.
Results: T-Ad ($r = 0.315$, $p = 0.022$) and HMW-Ad levels ($r = 0.338$, $p = 0.013$) were positively associated with subcutaneous fat area evaluated by performing CT scan at term-equivalent age, but were not associated with visceral fat area in simple regression analyses. In addition, T-Ad ($\beta = 0.487$, $p = 0.003$) and HMW-Ad levels ($\beta = 0.602$, $p < 0.001$) were positively associated with subcutaneous fat tissue area, but they were not associated with visceral fat area also in multiple regression analyses.
Conclusion: Subcutaneous fat accumulation contributes to increased levels of T-Ad and HMW-Ad, while visceral fat accumulation does not influence adiponectin levels in preterm infants at term-equivalent age.

1. Introduction

The hormone adiponectin is secreted exclusively by adipocytes and has a beneficial role in insulin sensitivity. Decreased production of adiponectin is associated with type 2 diabetes [1] and obesity [2], and especially with visceral fat accumulation in adults [3] and children [4]. Since high-molecular-weight adiponectin (HMW-Ad) is one of the active adiponectin multimers [5], HMW-Ad is reported to be a better marker of obesity-related complications than total adiponectin (T-Ad) [6]. In addition, the ratio of HMW-Ad to T-Ad (HMW%) is also significantly associated with insulin resistance [7].

Low birth weight infants have an increased risk of adult-onset diseases, including type 2 diabetes mellitus, cardiovascular disease, and obesity [8]. Not only small for gestational age (SGA) infants, but also low birth weight infants (caused by preterm birth) have a higher risk of insulin resistance in later life than term-appropriate for gestational age (AGA) infants [9], although the mechanisms have yet to be fully elucidated [10]. A recent investigation has shown that preterm infants have altered adiponectin levels, including decreased HMW% at term-equivalent age compared with term infants at birth [11]; this effect is present even if the infant does not present with extra-uterine growth restriction (EUGR) [12]. In addition, preterm infants have a higher percentage of fat mass [13] and increased volume of visceral fat [14], which may influence adiponectin production at term-equivalent age.

Some previous investigations have suggested that postnatal growth, as indicated by rate of weight gain [15] or body weight standard deviation (SD) score for example, increases from birth to term-equivalent age [12] and is one of the significant predictors of the increases in T-Ad and HMW-Ad levels in preterm infants during this period. These results indicate that fat tissue accumulation during this period may increase adiponectin production (the opposite effect of that in children and adults with obesity). However, growth during the postnatal period results from fat tissue accumulation; in addition, 'true' growth also occurs, such as increases in muscle mass, body length, and head circumference. Hence, it remains unclear whether fat tissue accumulation really depends on an increase in the levels of T-Ad and HMW-Ad in preterm infants during this period because no information regarding the direct association between fat tissue accumulation and adiponectin levels in preterm infants at term-equivalent age is available. Moreover, it also remains unknown how the fat distribution influences T-Ad and HMW-Ad levels in preterm infants at term-equivalent age.

Hence, in this study, we measured serum T-Ad and HMW-Ad levels and investigated visceral fat area (VFA) and subcutaneous fat area (SFA), using commercially available software; we were able to calculate the values from a fat density evaluation by computed tomography (CT) scan at the levels of the umbilicus. Our aim was to clarify whether the amount of fat tissue is correlated with T-Ad and HMW-Ad levels in preterm infants at term-equivalent age and whether visceral fat accumulation influences the levels of T-Ad and HMW-Ad in preterm infants at term-equivalent age.

* Corresponding author at: Department of Pediatrics, Showa University School of Medicine, 1-5-8 Hatanodai, Shinagawa-ku, Tokyo 142-8666, Japan. Tel.: +81 3 3784 8677; fax: +81 3 3784 7410.
E-mail address: nakano_yt_tulip@yahoo.co.jp (Y. Nakano).

http://dx.doi.org/10.1016/j.earlhumdev.2014.02.009
0378-3782/

2. Methods

2.1. Subjects

The Ethics Committee at Showa University School of Medicine approved the study protocol, and we obtained written informed consent from the subjects' parents. The study subjects were 53 preterm infants (23 male and 30 female), born at 24–34 weeks of gestation. All the infants were recruited from Showa University School of Medicine between August 1, 2010 and May 3, 2012. The subjects in the present study were part of a population in which we had already studied adiponectin levels in term and preterm infants. We have reported the clinical profile of the preterm subjects and their mothers in detail [12]. We obtained written informed consent for the CT scan in this study from 53 subjects among 58 preterm subjects in the previous study (that is, 5 parents of other subjects declined the CT scan). The subjects include 7 SGA infants, defined as birth weight <−2 SD and also include 5 EUGR at term-equivalent age, defined as body weight <−2 SD at term-equivalent age. All subjects were fed breast milk and infant formula. Breast milk was fortified for all subjects with a birth weight of less than 1500 g. Parenteral amino acids, which amounted to 1.5–2.5 $g \cdot kg^{-1} \cdot day^{-1}$, were administered as soon as possible after birth to all subjects whose birth weight was <1700 g. No subject whose birth weight was >1700 g received support with parenteral amino acids.

2.2. Measurement of VFA and SFA in CT scan

Visceral and subcutaneous fat volumes were evaluated by measuring VFA and SFA determined in a CT scan image, by using commercially available software (Virtual Place Advance; AZE, Ltd, Tokyo, Japan). All subjects were examined in the supine position. A single slice of cross-sectional CT scan (LightSpeed; GE Healthcare Japan Co., Tokyo, Japan) was performed at the level of the umbilicus (from L4 to L5). The software automatically defined a region of interest by tracking its contour on each scan, and the attenuation range of CT values (in Hounsfield units) for fat tissue was calculated. A histogram for fat tissue was automatically computed by the software on the basis of mean attenuation ± 1 SD. Tissue with attenuation values within the mean ± 1 SD was considered to be fat tissue on the basis of a previously reported concept [16] within that region of interest. Trained radiologists made manual adjustments if needed, choosing a midway point between adipose and non-adipose tissue peaks when the peaks had considerable overlap and misclassification could occur [17]. The software automatically divided total fat area into SFA and VFA, and radiologists also made manual adjustments if needed. To test the variability of SFA and VFA, the inter-observer and intra-observer coefficients for all 53 subjects were calculated. The inter-observer intraclass correlation coefficient for SFA and VFA was 0.980 and 0.956 (coefficient variation (CV), 3.8% and 9.1%), respectively. To assess intra-observer variability, the same observer repeated the adjustment of measurements of SFA and VFA on two different occasions. The intra-observer intraclass correlation coefficient for SFA and VFA was 0.992 and 0.982 (CV, 2.4% and 5.6%). The ratio of VFA to SFA was designated as the V/S ratio.

2.3. Anthropometric measurements

Physical measurements such as body weight and length were determined immediately by experienced nurses after birth and at term-equivalent age. The medical records of the subjects were reviewed retrospectively. Body weight was measured by using a standard electronic scale. Body weight SD scores for gestational age were determined according to Japanese reference data [18], which were differentiated by sex, number of deliveries, and gestational days. Their mother's body weight and height before pregnancy were self-reported. Body mass index (BMI) was calculated as body weight/length^2 (kg/m^2).

2.4. Measurements of T-Ad, HMW-Ad, and leptin

To determine serum T-Ad, HMW-Ad, and leptin, blood samples were collected from the dorsum manus vein 2 or 3 h after feeding in preterm infants at term-equivalent age. Sera for the assays were obtained by centrifugation of the blood samples and were immediately frozen. The specimens were stored at −40 °C before analysis. Serum T-Ad and HMW-Ad concentrations were determined by ELISA using a commercial kit (Daiichi Pure Chemicals, Tokyo, Japan), and serum leptin levels were measured using a commercial RIA kit (Linco Research, St Louis, MO, USA). The intra-assay variation (CV) for the T-Ad and HMW-Ad assays was 5.3% and 3.3%, as described previously [19], and that of the leptin assay was <8%. HMW% was calculated as (HMW-Ad / T-Ad) × 100.

2.5. Statistical analyses

All analyses were performed with the Statistical Package for the Social Sciences (SPSS) Statistics Desktop for Japan Version 19.0 (IBM Company, Tokyo, Japan). We used the Mann–Whitney test to compare adiponectin levels between male and female infants or between 19 very preterm infants born before 32 weeks and 34 other preterm infants born at 32 weeks gestation or more. We evaluated the correlation of SFA, VFA, and V/S ratio to other variables by using bivariate Pearson's correlation in a simple linear regression and a model of multiple regression analysis. In addition, we also evaluated the influence of an amount and distribution of fat tissue on T-Ad, HMW-Ad, HMW%, and leptin, in the same way. Multiple regression analyses were performed to assess the influence of multiple variables such as SFA, VFA, sex, gestational age, and body weight SD score at term-equivalent age on serum T-Ad, HMW-Ad, HMW%, and leptin at term-equivalent age; we excluded birth weight and body weight at term-equivalent age from the dependent variables because they are strongly correlated with other factors such as gestational age. The associations were considered statistically significant when the p values were <0.05.

3. Results

The clinical characteristics of the subjects are shown in Table 1. The mean birth weight, birth weight SD score, and gestational age were 1592 g, −0.7 SD, and 32.1 weeks, respectively. The mean body weight, body weight SD score, and age of the subjects at term-equivalent age were 2737 g, −0.8 SD, and 39.3 weeks. The subjects included 5 infants that presented with EUGR, defined as body weight SD score <−2 SD at term-equivalent age. The mean SFA, VFA, and V/S ratio evaluated at term-equivalent age were 9.4 cm^2, 3.4 cm^2, and 0.39, respectively. The mean levels of T-Ad, HMW-Ad, and HMW% measured at term-equivalent age were 22.8 μg/mL, 13.7 μg/mL, and 59.3%, respectively. T-Ad and HMW-Ad levels were significantly higher in

Table 1
Clinical characteristics of the study subjects.

Number of subjects (male/female)	N = 53 (23/30)	
	Mean ± SD	Median (range)
Maternal age (years)	33.2 ± 5.1	33.0 (26.1–49.0)
Maternal BMI before pregnancy (kg/m^2)	21.1 ± 3.1	20.0 (16.8–30.8)
At birth		
Gestational age (weeks)	32.1 ± 2.7	33.3 (26.3–34.9)
Birth weight (g)	1592 ± 499	1611 (659–2519)
Birth weight SD score	−0.7 ± 1.0	−0.7 (−3.5–1.2)
BMI (kg/m^2)	9.3 ± 1.5	9.0 (6.4–12.7)
At term-equivalent age		
Gestational age (weeks)	39.3 ± 1.2	39.3 (37.3–41.9)
Body weight (g)	2737 ± 354	2684 (2219–3846)
Body weight SD score	−0.8 ± 0.9	−0.7 (−2.9–1.4)
BMI (kg/m^2)	12.2 ± 1.4	11.8 (10.2–17.1)
T-Ad (μg/mL)	22.8 ± 7.6	21.6 (10.0–41.9)
HMW-Ad (μg/mL)	13.7 ± 5.3	13.6 (4.5–31.0)
HMW% (%)	59.3 ± 8.6	58.7 (41.5–81.8)
Leptin (ng/mL)	2.3 ± 0.8	2.2 (0.7–4.2)
Subcutaneous fat tissue area (cm^2)	9.4 ± 3.6	9.2 (2.7–18.6)
Visceral fat tissue area (cm^2)	3.4 ± 2.5	2.9 (0.1–11.4)
V/S ratio	0.39 ± 0.27	0.34 (0.01–1.07)

BMI: Body mass index, SD: standard deviation; T-Ad: total adiponectin; HMW-Ad: high-molecular-weight adiponectin; HMW%: ratio of HMW-Ad to T-Ad; V/S ratio: the ratio of visceral to subcutaneous fat tissue area.

female subjects than in male subjects (T-Ad: 20.3 ± 5.7 μg/mL in male subjects versus 24.8 ± 8.4 μg/mL in female subjects, $p = 0.018$; HMW-Ad: 12.2 ± 3.9 μg/mL in male subjects versus 14.9 ± 5.9 μg/mL in female subjects, $p = 0.007$). Nineteen very preterm infants born before 32 weeks of gestation had significantly larger SFA and lower (although not significantly lower) adiponectin levels than 34 preterm infants born at 32 weeks of gestation or more (SFA: 11.8 ± 4.0 cm^2 for very preterm infants versus 8.0 ± 2.6 cm^2 for the other preterm infants, $p = 0.007$; T-Ad: 21.6 ± 7.9 μg/mL for the very preterm infants versus 23.6 ± 7.5 μg/mL for the other preterm infants; HMW-Ad: 12.5 ± 5.1 μg/mL for the very preterm infants versus 14.4 ± 5.3 μg/mL for the other preterm infants).

In a simple regression analysis, SFA was inversely associated with gestational age ($r = -0.456$, $p < 0.001$) and positively associated with the age in the subjects at term-equivalent age ($r = 0.335$, $p = 0.014$), body weight at term-equivalent age ($r = 0.578$, $p < 0.001$), body weight SD score at term-equivalent age ($r = 0.502$, $p < 0.001$), and BMI at term-equivalent age ($r = 0.561$, $p < 0.001$), although it was not significantly associated with other variables including birth weight, birth weight SD score, maternal age, and maternal BMI before pregnancy. Conversely, VFA was negatively associated only with gestational age ($r = -0.281$, $p = 0.049$), and V/S ratio was associated only with body weight at term-equivalent age ($r = -0.278$, $p = 0.044$) (data not shown). In the multiple regression analyses performed to identify independent predictors of SFA, VFA, and V/S ratio in the subjects at term-equivalent age considering sex, gestational age, birth weight SD score, and the age and body weight SD score at term-equivalent age, SFA had a positive association with body weight SD score ($\beta = 0.474$, $p = 0.001$) and the age ($\beta = 0.285$, $p = 0.023$) at term-equivalent age and negative association with gestational age ($\beta = -0.323$ $p = 0.007$) (adjusted $R^2 = 0.455$, $p < 0.001$). There were no significant predictors of VFA and V/S ratio (data not shown).

With regard to the association of fat distribution and accumulation with T-Ad, HMW-Ad, HMW%, and leptin levels at term-equivalent age, T-Ad ($r = 0.315$, $p = 0.022$), HMW-Ad ($r = 0.338$, $p = 0.013$), HMW% ($r = 0.273$, $p = 0.048$), and leptin ($r = 0.297$, $p = 0.031$) were positively associated with SFA, but were not associated with VFA and V/S ratio in the simple regression analyses (data not shown). The significant associations for T-Ad, HMW-Ad, and HMW% were strengthened after adjustment for variables including sex, gestational age, birth weight, birth weight SD score, BMI at birth, maternal age, maternal BMI before pregnancy, and the age, body weight, body weight SD score, and BMI at term-equivalent age (T-Ad: $r = 0.521$, $p < 0.001$; HMW-Ad: $r = 0.628$, $p < 0.001$; and HMW%: $r = 0.476$, $p = 0.001$), although the significance for leptin disappeared after adjustment. In the multiple regression analyses performed to identify independent predictors of T-Ad, HMW-Ad, HMW%, and leptin levels at term-equivalent age, sex, gestational age, SFA, VFA, and body weight SD score at term-equivalent age were considered as potential predictors. T-Ad and HMW-Ad had significant positive associations with SFA (T-Ad: $\beta = 0.487$ $p = 0.003$, HMW-Ad: $\beta = 0.602$ $p < 0.001$), female sex (T-Ad: $\beta = 0.408$ $p = 0.001$, HMW-Ad: $\beta = 0.364$ $p = 0.002$), and gestational age (T-Ad; $\beta = 0.557$, $p < 0.001$, HMW-Ad; $\beta = 0.607$, $p < 0.001$), as shown in Table 2. If the 7 SGA infants are excluded, the results relating to the association between T-Ad or HMW-Ad and SFA or VFA remain the same. The addition of maternal age or/and BMI before pregnancy as confounding factors did not give more strength in this relationship between adiponectin and SFA at term-equivalent age. With regard to HMW%, the regression formula was not significant (adjusted $R^2 = 0.111$, $p = 0.060$). Although the leptin levels were positively associated with SFA ($\beta = 0.361$ $p = 0.043$) and female sex ($\beta = 0.335$ $p = 0.014$), the significance level in the regression formula was not strong (adjusted $R^2 = 0.188$, $p = 0.010$).

4. Discussion

In adults and children, BMI has a paradoxical negative association with serum adiponectin levels, although adiponectin is exclusively produced by adipocytes, and obesity is related to decreased adiponectin levels even in children [4]. In neonates, on the other hand, cord serum adiponectin is positively related to birth weight and gestational age [20,21], suggesting that fetal growth in utero including fat tissue may contribute to increased adiponectin production. The reason for this inconsistency regarding the association between fat tissue accumulation and adiponectin levels remains unclear; however, it has been hypothesized that the difference might be related to a lack of negative feedback on adiponectin production associated with a lack of fat cell hypertrophy [20]. With regard to preterm infants from birth to term-equivalent age, some previous studies suggested that postnatal growth during this period contributed to the increases in T-Ad and HMW-Ad [12,15]. However, no previous reports have directly investigated the association between adipose tissue accumulation and adiponectin levels in preterm infants at term-equivalent age. The present study suggests that subcutaneous fat accumulation contribute to increased levels of T-Ad and HMW-Ad.

One possible explanation for the association seen here between adiponectin levels and SFA is that increased volumes of subcutaneous fat tissue between birth and term-equivalent age in preterm infants may be the result of increased numbers of small differentiated adipocytes, as speculated in a previous study [15]. This is because fat cell hypertrophy is associated with decreased adiponectin expression in adipocytes [22]. On the other hand, the present study also indicates that very preterm infants may have increased levels of subcutaneous fat and comparatively low levels of T-Ad and HMW-Ad at term-equivalent age compared with more mature preterm infants. In term infants, adipose tissue rapidly expands, mainly as a result of the increased number of small adipocytes present during the second half of fetal life, and this is probably associated with the drastically increased adiponectin levels seen during this period. Fat cells enlarge during the first 12 months of life after birth, while the number of fat cells remains unchanged [23]. If we apply this to preterm infants, fat cell hypertrophy might occur, to a certain degree, in very preterm infants, while fat cell numbers increase between birth and term-equivalent age and hypertrophy may induce comparatively low T-Ad and HMW-Ad levels in very preterm infants at term-equivalent age. This hypothesis is, however, not supported by sufficient data, and further study is necessary to investigate the size and number of fat cells in preterm infants at term-equivalent age.

Some observational studies have shown that visceral fat accumulation is one of the important factors for development of insulin resistance and its co-morbidities in adults and children [24,25]. This is considered to be partly because visceral fat accumulation is associated with decreased HMW-Ad production [3,4]. Conversely, some previous investigations have shown that subcutaneous fat tissue rather than visceral fat tissue was inversely associated with serum adiponectin levels in healthy and relatively lean young men [26] and in overweight and obese men [27]. Because a previous study reported an increased volume of visceral fat in preterm infants at term-equivalent age [14], we hypothesized that visceral fat accumulation influenced levels of adiponectin in preterm infants at term-equivalent age. However, the present study failed to show the association between visceral fat accumulation and adiponectin levels including T-Ad, HMW-Ad, and HMW% in preterm infants at term-equivalent age. These results imply that altered adiponectin levels in preterm infants at term-equivalent age may be induced by an alternative pathogenesis other than visceral fat accumulation.

Our results suggest that there is a sex effect on adiponectin levels in preterm infants at term-equivalent age. Adiponectin concentration is consistently lower in male than in female subjects (at least in adolescents), and this is probably influenced by sex hormones [28]. Sex differences in adiponectin levels are seen in the fetus but not in term infants at birth [29]. One possible explanation for our results is that elevated testosterone levels might influence adiponectin levels in male preterm infants, although we did not measure testosterone in the present study. A previous investigation found a prolonged increase in testosterone levels, with peak testosterone levels at 3–4 months of age, and a slower decrease in testosterone levels in preterm male infants compared with term-born male infants [30].

We found a significant positive association between subcutaneous fat accumulation and leptin levels at term-equivalent age in preterm infants, although this association is not highly significant. This is consistent with a previous report suggesting a significant positive association between leptin levels and subscapular skinfold thickness determining central subcutaneous fat deposition in preterm infants within 4 weeks after birth, although the same report suggested a significant inverse association between leptin levels and triceps or mid-thigh skinfold thickness determining peripheral subcutaneous fat deposition [31].

This study has some limitations. First, the small sample size means that the study does not have sufficient statistical power to evaluate the association between fat tissue accumulation or distribution and adiponectin levels in preterm infants at term-equivalent age; hence, the results should be confirmed in a larger population. Second, there is no information on the accuracy of adipose tissue evaluated by performing CT scan in neonates, to the best of our knowledge. Regions of interest are usually a representative area containing both adipose tissue and bordering tissues or air in the evaluations of subcutaneous and visceral fat mass by CT scan [17]. Neonatal infants have very small amount of subcutaneous and visceral fat tissue and a relatively large amount of bowel gas compared with adults and children, and these differences might influence the evaluations of SFA and VFA in the present study.

In conclusion, our results suggest that subcutaneous fat accumulation, but not visceral fat accumulation, is associated with increased production of T-Ad and HMW-Ad in preterm infants at term-equivalent age. There may be a different mechanism(s) for control of adiponectin production in visceral and subcutaneous fat during adipose tissue development in preterm infants compared with that in adults and children with obesity.

Please cite this article as: Nakano Y, et al, Accumulation of subcutaneous fat, but not visceral fat, is a predictor of adiponectin levels in preterm infants at term-equivalent..., Early Hum Dev (2014), http://dx.doi.org/10.1016/j.earlhumdev.2014.02.009

Table 2
Multiple regression analysis of factors related to serum T-Ad, HMW-Ad, HMW%, and leptin in preterm infants at term-equivalent age.

Variables	Serum levels at term-equivalent age							
	T-Ad[a]		HMW-Ad[b]		HMW%[c]		Leptin[d]	
	β[e]	p	β[e]	p	β[e]	p	β[e]	p
Gestational age (weeks)	**0.557**	**<0.001**	**0.607**	**<0.001**	**0.402**	**0.013**	0.203	0.181
Sex (male)	**−0.408**	**0.001**	**−0.364**	**0.002**	0.002	0.991	**−0.335**	**0.014**
Body weight SD score at term-equivalent age	0.119	0.545	−0.047	0.963	−0.130	0.418	0.123	0.424
Subcutaneous fat tissue area (cm^2)	**0.487**	**0.003**	**0.602**	**<0.001**	**0.528**	**0.006**	**0.361**	**0.043**
Visceral fat tissue area (cm^2)	−0.041	0.730	−0.077	0.512	−0.024	0.868	−0.236	0.086

Bold type indicates significant correlations.
T-Ad: total adiponectin; HMW-Ad: high-molecular-weight adiponectin; HMW%: ratio of HMW-Ad to T-Ad; SD: standard deviation.
[a] Adjusted $R^2 = 0.373$, $p < 0.001$.
[b] Adjusted $R^2 = 0.396$, $p < 0.001$.
[c] Adjusted $R^2 = 0.111$, $p = 0.060$.
[d] Adjusted $R^2 = 0.188$, $p = 0.010$.
[e] β was standardized.

Conflict of interest

We declare that no financial support or relationship will pose a conflict of interest.

Acknowledgments

This work was supported by JSPS KAKENHI Grant Number 22591208. The authors thank the babies and their parents for participating in this study.

References

[1] Spranger J, Kroke A, Möhlig M, Bergmann MM, Ristow M, Boeing H, et al. Adiponectin and protection against type 2 diabetes mellitus. Lancet 2003;361:226–8.
[2] Arita Y, Kihara S, Ouchi N, Takahashi M, Maeda K, Miyagawa J, et al. Paradoxical decrease of an adipose-specific protein adiponectin in obesity. Biochem Biophys Res Commun 1999;257:79–83.
[3] Saito T, Murara M, Otani T, Tamemoto H, Kawakami M, Ishikawa SE. Association of subcutaneous and visceral fat mass with serum concentrations of adipokines in subjects with type 2 diabetes mellitus. Endocr J 2012;59:39–45.
[4] Asayama K, Hayashibe H, Dobashi K, Uchida N, Nakane T, Kodera K, et al. Decrease in serum adiponectin level due to obesity and visceral fat accumulation in children. Obes Res 2003;11:1072–9.
[5] Hada Y, Yamauchi T, Waki H, Tsuchida A, Hara K, Yago H, et al. Selective purification and characterization of adiponectin multimer species from human plasma. Biochem Biophys Res Commun 2007;356:487–93.
[6] Araki S, Dobashi K, Kubo K, Asayama K, Shirahara A. High molecular weight, rather than total adiponectin levels better reflect metabolic abnormalities associated with childhood obesity. J Clin Endocrinol Metab 2006;91:5113–6.
[7] Aso Y, Yamamoto R, Wakabayashi S, Uchida T, Takayanagi K, Okuno T, et al. Comparison of serum high-molecular weight (HMW) adiponectin with total adiponectin concentrations in type 2 diabetic patients with coronary artery disease using a novel enzyme-linked immunosorbent assay to detect HMW adiponectin. Diabetes 2006;55:1954–60.
[8] Gluckmann PD, Hanson MA, Cooper C, Thornburg KL. Effects of in utero and early-life conditions on adult health and disease. N Engl J Med 2008;359:61–73.
[9] Hofman PL, Regan F, Jackson WE, Jefferies C, Knight DB, Robinson EM, et al. Premature birth and later insulin resistance. N Engl J Med 2004;351:2179–86.

Please cite this article as: Nakano Y, et al, Accumulation of subcutaneous fat, but not visceral fat, is a predictor of adiponectin levels in preterm infants at term-equivalent..., Early Hum Dev (2014), http://dx.doi.org/10.1016/j.earlhumdev.2014.02.009

[10] Lapillonne A, Griffin IJ. Feeding preterm infants today for later metabolic and cardiovascular outcomes. J Pediatr 2013;162:S7–S16.
[11] Yoshida T, Nagasaki H, Asato Y, Ohta T. The ratio of high-molecular weight adiponectin and total adiponectin differs in preterm and term infants. Pediatr Res 2009;65:580–3.
[12] Nakano Y, Itabashi K, Sakurai M, Aizawa M, Dobashi K, Mizuno K. Preterm infants have altered adiponectin levels at term-equivalent age even if they do not present with extrauterine growth restriction. Horm Res Paediatr 2013;80:147–53.
[13] Atkinson SA, Randall-Simpson J. Factors influencing body composition of premature infants at term-adjusted age. Ann N Y Acad Sci 2000;904:393–9.
[14] Uthaya S, Thomas EL, Hamilton G, Dore CJ, Bell J, Modi N. Altered adiposity after extremely preterm birth. Pediatr Res 2005;57:211–5.
[15] Saito M, Nishimura K, Nozue H, Miyazono Y, Kamoda T. Changes in serum adiponectin levels from birth to term-equivalent age are associated with postnatal weight gain in preterm infants. Neonatology 2011;100:93–8.
[16] Yoshizumi T, Nakamura T, Yamane M, Islam AH, Menju M, Yamasaki K, et al. Abdominal fat: standardized technique for measurement at CT. Radiology 1999;211:283–6.
[17] Van der Kooy K, Seidell JC. Techniques for the measurement of visceral fat: a practical guide. Int J Obes Relat Metab Disord 1993;17:187–96.
[18] Itabashi Kazuo. Standard values of birth weight, length, and head circumstances at birth. [in Japanese] Perinat Med 2010;40(special issue):943–60 [Tokyo].
[19] Ebinuma H, Miyazaki O, Yago H, Hara K, Yamauchi T, Kadowaki T. A novel ELISA system for selective measurement of human adiponectin multimers by using proteases. Clin Chim Acta 2006;372:47–53.
[20] Sivan E, Mazaki-Tovi S, Pariente C, Efraty Y, Schiff E, Hemo R, et al. Adiponectin in human cord blood: relation to feral birth weight and gender. J Clin Endocrinol Metab 2003;88:5656–60.
[21] Kajanite E, Hytinantti T, Hovi P, Andersson S. Cord plasma adiponectin: a 20-fold rise between 24 weeks gestation and term. J Clin Endocrinol Metab 2004;89:4031–6.
[22] Ito A, Suganami T, Miyamoto Y, Yoshimasa Y, Takeya M, Kamei Y, et al. Role of MAPK phosphatase-1 in the induction of monocyte chemoattractant protein-1 during the course of adipocyte hypertrophy. J Biol Chem 2007;282:25445–52.
[23] Kiess W, Petzold S, Töpfer M, Garten A, Blüher S, Kapellen T, et al. Adipocytes and adipose tissue. Best Pract Res Clin Endocrinol Metab 2008;22:135–53.
[24] Fujimoto WY, Bergstorm RW, Byoko EJ, Chen KW, Leonetti DL, Newell-Morris L, et al. Visceral adiposity and incident coronary heart disease in Japanese-American men. The 10-year follow-up results of the Seattle Japanese-American Community Diabetes Study. Diabetes Care 1999;22:1808–12.
[25] Taksali SE, Caprin S, Dziura J, Dufour S, Cali AM, Doodman TR, et al. High visceral and low abdominal subcutaneous fat stores in the obese adolescent: a determinant of an adverse metabolic phenotype. Diabetes 2008;57:367–71.
[26] Frederiksen L, Nielsen TL, Wraae K, Hagen C, Frystyk J, Flyvbierg A, et al. Subcutaneous rather than visceral adipose tissue is associated with adiponectin levels and insulin resistance in young men. J Clin Endocrinol Metab 2009;94:4010–5.
[27] Farvid MS, Ng TW, Chan DC, Barrett PH, Watts GF. Association of adiponectin and resistin with adipose tissue compartments, insulin resistance and dyslipidemia. Diabetes Obes Metab 2005;7:406–13.
[28] Riestra P, Garcia-Anguita A, Ortega L, Garcés C. Relationship of adiponectin with sex hormone levels in adolescents. Horm Res Paediatr 2013;79:83–7.
[29] Kajantie E, Hytinantti T, Hovi P, Andersson S. Cord plasma adiponectin: a 20-fold rise between 24 weeks gestation and term. J Clin Endocrinol Metab 2004;89:4031–6.
[30] Tapanainen J, Koivisto M, Vihko R, Huhtaniemi I. Enhanced activity of the pituitary–gonadal axis in premature human infants. J Clin Endocrinol Metab 1981;52:235–8.
[31] Moyer-Mileur LJ, Haley S, Slater H, Beachy J, Smith SL. Massage improves growth quality by decreasing body fat deposition in male preterm infants. J Pediatr 2013;162:490–5.

Please cite this article as: Nakano Y, et al, Accumulation of subcutaneous fat, but not visceral fat, is a predictor of adiponectin levels in preterm infants at term-equivalent..., Early Hum Dev (2014), http://dx.doi.org/10.1016/j.earlhumdev.2014.02.009

PEDIATRICS INTERNATIONAL Official Journal of the Japan Pediatric Society

Pediatrics International (2014) **56**, 702–708 doi: 10.1111/ped.12331

Original Article

New Japanese neonatal anthropometric charts for gestational age at birth

Kazuo Itabashi,[1] Fumihiro Miura,[1] Ritei Uehara[2] and Yoshikazu Nakamura[2]

[1]*Department of Pediatrics, Showa University School of Medicine, Tokyo and* [2]*Department of Public Health, Jichii Medical University, Tochigi, Japan*

Abstract ***Background***: More than 10 years have passed since the previous Japanese neonatal growth charts were published, therefore the aim of this study was to develop an updated set of Japanese neonatal growth charts.

Methods: We used data from the registry database of the Japan Society of Obstetrics and Gynecology from 2003 until 2005. A total of 150 471 singleton live births without stillbirth or severe congenital malformation were enrolled in the preliminary analysis. It was found that the distribution of the 10th centile charts based on these subjects was skewed toward lower birthweight for preterm infants, because of the significantly lower birthweight in the 10th centile in neonates delivered by cesarean section than those delivered vaginally. Therefore, the data of subjects delivered by cesarean section were also excluded.

Results: Finally, 104 748 singleton vaginal births at 22–41 weeks of gestation were used to construct a new set of Japanese neonatal anthropometric charts. The birthweight chart is parity and sex specific. The differences between the Japanese fetal growth chart and the new neonatal birthweight chart were small.

Conclusion: The present new neonatal anthropometric charts may reveal unrestricted growth pattern mimicking fetal growth. Use of these charts may result in recognition of abnormal fetal growth and risk in preterm infants. Further studies are needed to evaluate the risk for adverse neonatal and long-term outcome among small-for-gestational-age infants using these neonatal charts.

Key words delivery mode, growth chart, Japanese, neonate, small for gestational age.

A neonatal anthropometric chart for determining gestational age at birth, called a neonatal growth chart, is an essential tool for identifying neonates at higher risk of neonatal or postnatal morbidity and fetal growth impairment, as well as for monitoring postnatal growth in preterm infants. A secular trend in neonatal anthropometric measurements at birth is associated with changes not only in antenatal management and maternal age and size but also in socioeconomic or environmental conditions.[1] Therefore, neonatal growth charts should be updated accordingly. The neonatal growth charts published during the last decade have improved on earlier charts by using more appropriate methods and more current, larger, diverse samples of infants.[2–6]

The Japanese neonatal growth chart, which was revised in 1995, has been widely used by Japanese obstetricians and pediatricians for managing pregnancy and newborns.[7] Given that more than 10 years had passed since the revised charts were published, the research committee of the Ministry of Health, Welfare, and Labor for Multicenter Benchmark Research on Neonatal Outcomes in Japan decided to develop a new Japanese growth chart. The goal of this study was to develop a new set of Japanese neonatal growth charts (including birthweight, body length, and head circumference).

Correspondence: Kazuo Itabashi, MD PhD, Department of Pediatrics, Showa University School of Medicine, 1-5-8 Hatanodai, Shinagawa-ku, Tokyo 142-8666, Japan. Email: kitaba@med.showa-u.ac.jp

Received 21 August 2013; revised 30 January 2014; accepted 4 February 2014.

Methods

Data collection

To create a new set of neonatal growth charts, we used the registry database of the Japan Society of Obstetrics and Gynecology (JSOG). This database included 147 medical facilities (level II and III) that participated in the JSOG registry system. Not only are low-risk infants cared for in normal newborn nurseries or by rooming-in, but also high-risk infants are cared for in neonatal intensive care units in these facilities. This registry system was managed by the committee of perinatal medicine of JSOG. Data were collected using an online system and stored in JSOG. Data from this database were collected from 2003 until 2005 on gestational age, birthweight, sex, birth order, and information on complications of singleton births. Gestational age, recorded in completed weeks and days, was primarily based on ultrasonography results within the first trimester. Because JSOG approved the use of their database for creating new neonatal growth charts, this study was not subject to institutional review.

Preliminary analysis

During the study period, 150 471 singleton births were reported in the registry database. Stillborn infants and those with severe asphyxia (Apgar score of 0 at 1 and 5 min after delivery), hydrops fetalis, or severe congenital malformations were excluded from the analysis. Infants with missing information on sex or gestational age were also excluded. We conducted a preliminary analysis for 144 980 infants. As previously reported by Uehara *et al.*, the distribution of 10th centile charts was skewed toward lower birthweight for preterm infants, and large differences in 10th-centile birthweight were observed between newborn infants delivered vaginally and those by cesarean section during the preterm period.[8] Approximately 63% of boys and 58% of girls were delivered by cesarean section at <37 weeks of gestation (Table 1). Indications for cesarean section were not available in the JSOG registration database. The maximum difference in birthweight at the 10th centile between the growth chart based on the overall sample and the previous Japanese chart[7] was approximately 400 g during the preterm period (Fig. 1). The 10th-centile birthweight in preterm infants decreased during 2003–2005 compared to that during 1995; this decrease of birthweight is a secular trend in Japan. This may be mainly explained by changes in obstetric intervention in preterm infants with fetal growth restriction (FGR). Therefore, we decided to exclude newborn infants delivered by cesarean section from analysis.

Creation of smoothed percentile charts

Finally, data from 104 748 singleton births delivered vaginally at 22–41 weeks of gestation were used to construct a new set of Japanese neonatal anthropometric charts using Cole's lambda mu sigma (LMS) method, which is regarded as the gold standard for tracing anthropometric charts.[9] Among 104 748 infants, there were missing data on body length and head circumference at birth. Body length and head circumference charts were constructed using data from 89 775 infants and 38 603 infants, respectively. LMSChartMaker Pro 2.324 (Medical Research Council, London, UK) was used to create smoothed percentile charts for the 3rd, 10th, 50th, 90th, and 97th percentiles from these raw data.

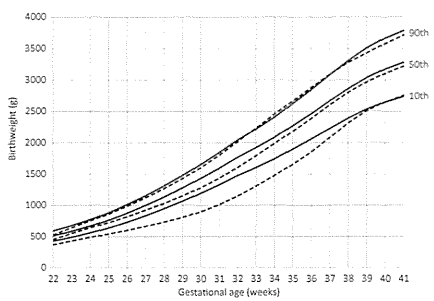

Fig. 1 Comparison between (—) the previous birthweight chart for male primiparous infants and (- - -) the present chart including the entire male, primiparous subject group. The maximum difference in birthweight at the 10th centile was approximately 400 g during the preterm period.

LMS method

According to Cole, the LMS method provides a way of obtaining normalized growth centile standards, which simplifies this assessment, and which deals generally with skewness that may be present in the distribution of the measurement.[9] It assumes that the data can be normalized by using a power transformation, which stretches one tail of the distribution and shrinks the other, removing the skewness. The optimal power to obtain normality is calculated for each of a series of age groups and the trend summarized by a smooth (L) curve. Trends in the mean (M) and coefficient of variation (S) are similarly smoothed.

L, M and S correspond to the following formulas: $Z = [(X/M)^{L} - 1]/LS$, where X is the measured value of weight, length, or head circumference; and centile = $M(1 + LSZ)^{1/L}$, where Z is the z score that corresponds to a given percentile. Z score is a measure of the distance in standard deviations of a sample from the mean. Corresponding Z values for 3rd, 10th, 50th, 90th and 97th percentiles are −1.88079, −1.28155, 0, 1.28155 and 1.88079, respectively.

Results

Centile charts for birthweight, length, and head circumference were created. Descriptive statistics and the LMS parameters for the new charts are presented in Tables 2–5. The birthweight centile chart was sex and parity specific. Because the effects of sex and parity on length and head circumference at birth were not significant, the growth charts for length and head circumference were not sex and parity specific, respectively. The equivalent degrees of freedom (e.d.f.) for L, M and S in birthweight centile charts were 3-5-3 and 3-5-3 for primiparous and multiparous in both genders, respectively. The e.d.f. for L, M and S in body length centile charts were 6-8-7 and those for head circumference were 3-6-4.

We compared the previous Japanese birthweight chart[7] with the new chart based on the vaginally delivered subjects. This previous chart was based on data from newborn infants delivered both vaginally and by cesarean section. The new birthweight chart is similar to the previous one. The Japanese fetal growth chart, which was not sex or parity specific, was derived from normal fetuses that proceeded to term delivery.[10] When we compared this fetal growth chart[10] at −1.5SD with the new neonatal

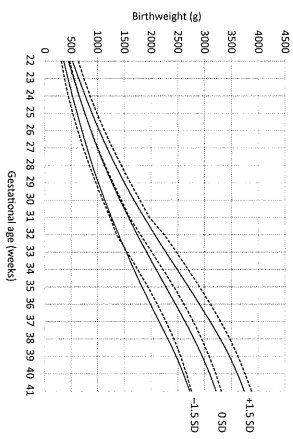

Fig. 2 (- - -) Fetal growth curves and (—) new birthweight curves (male, primiparous). (The fetal growth curves are not differentiated by sex and parity.) At −1.5SD, the differences are small up to 100 g.

chart at −1.5SD, these differences were small and up to 100 g (Fig. 2).

Discussion

We present a new set of Japanese neonatal anthropometric charts based on data from subjects born only by vaginal delivery. Approximately 60% of the overall subject group was delivered by cesarean section at <37 weeks of gestation (Table 1). In addition, the proportion of infants delivered by cesarean section at 26–29 weeks of gestation was approximately ≥75%, but we excluded the subjects delivered by cesarean section because of the large differences in birthweight at the 10th centile between subjects delivered vaginally and those by cesarean section during the preterm period.[8] Skjaerven *et al.* noted a clear decrease in birthweight for most of the preterm weeks from 1987 to 1998, which was related to the increase in cesarean section deliveries.[11] They agreed with Yudkin *et al.* that "it is illogical that changes in obstetric practice should alter the definition of an abnormally grown baby."[12] Therefore, they excluded the subjects delivered by cesarean section to provide a new standard for small-for-gestational-age (SGA) infants. We also agreed with Yudkin *et al.*[12] in this regard. A new set of Japanese neonatal anthropometric charts is also applicable to newborn infants delivered by cesarean section because these charts are used to evaluate growth status at birth for gestational age.

Owing to different inclusion criteria and the heterogeneity of methods used to trace growth charts, neonatal growth charts have wide differences in the cut-off values. The increasing trend toward obstetric intervention to hasten delivery for pathologic pregnancies during the preterm period, and in response to signs of slow growth, may continue to affect the shape of the anthropometric chart during the preterm period. Ananth and Vintzileos showed that ischemic placental disease such as pre-eclampsia, fetal distress, FGR, and placental abruption were implicated in well over half of all medically indicated preterm births in a population study in Missouri.[13] They concluded that

Table 1 No. subjects vs sex, delivery mode, and parity

Gestational age (weeks)	Male				Female			
	Primiparous		Multiparous		Primiparous		Multiparous	
	Cesarean section *n*	Vaginal delivery *n* (%)	Cesarean section *n*	Vaginal delivery *n* (%)	Cesarean section *n*	Vaginal delivery *n* (%)	Cesarean section *n*	Vaginal delivery *n* (%)
22	0	25 100	26	28 51.9	4	17 81.0	5	24 82.8
23	33	43 56.6	76	34 30.9	14	34 70.8	20	31 60.8
24	52	40 43.5	92	31 25.2	47	26 35.6	61	22 26.5
25	66	37 35.9	103	38 27.0	66	30 31.3	88	37 29.6
26	105	35 25.0	140	33 19.1	83	14 14.4	110	40 26.7
27	119	37 23.7	156	39 20.0	105	30 22.2	92	36 28.1
28	154	47 23.4	203	46 18.5	120	31 20.5	128	47 26.9
29	150	46 23.5	197	58 22.7	132	29 18.0	140	30 17.6
30	173	79 31.3	252	80 24.1	166	61 26.9	156	65 29.4
31	184	89 32.6	273	115 29.6	177	58 24.7	165	68 29.2
32	242	151 38.4	393	189 32.5	214	85 28.4	188	136 42.0
33	264	236 47.2	502	247 33.0	223	158 41.5	219	160 42.2
34	387	351 47.6	741	323 30.4	296	215 42.1	274	259 48.6
35	417	522 55.6	944	451 32.3	349	371 51.5	346	333 49.0
36	671	855 56.0	1537	772 33.4	586	642 52.3	635	623 49.5
37	1707	1993 53.9	3720	2246 37.6	1662	1623 49.4	2787	1753 38.6
38	1893	4748 71.5	6691	5147 43.5	1878	3841 67.2	2907	4488 60.7
39	1163	8454 87.9	9698	7660 44.1	1008	7723 88.5	570	7238 92.7
40	1354	7832 85.3	9271	5727 38.2	1129	8237 87.9	360	6362 94.6
41	1050	3360 76.2	4463	1735 28.0	963	3799 79.8	167	1993 92.3
Total	10184	28980 74.0	9798	24999 71.8	9222	27024 74.6	9418	23745 71.6

Table 2 Descriptive statistics and LMS parameters for male birthweight

Gestational age (weeks)	Day	Primiparous								Multiparous							
		L	M	S	3rd	10th	50th	90th	97th	L	M	S	3rd	10th	50th	90th	97th
22	0	1.59434	446.99500	0.12210	336	373	447	514	544	0.68161	449.38600	0.14979	329	366	449	538	581
23	0	1.56267	549.18550	0.12282	412	458	549	632	669	0.69573	552.12660	0.14922	404	450	552	661	713
24	0	1.53097	652.31130	0.12354	489	544	652	752	796	0.70991	656.89470	0.14864	481	535	657	785	848
25	0	1.49883	759.14110	0.12428	569	633	759	876	928	0.72435	766.49680	0.14803	562	625	766	916	988
26	0	1.46571	872.66940	0.12505	654	727	873	1008	1068	0.73947	883.06110	0.14737	648	721	883	1054	1136
27	0	1.43232	994.56200	0.12583	745	828	995	1150	1219	0.75554	1007.73600	0.14664	740	823	1008	1201	1295
28	0	1.40031	1125.61700	0.12664	842	936	1126	1303	1382	0.77282	1141.52000	0.14581	839	933	1142	1359	1464
29	0	1.37164	1266.00200	0.12742	947	1052	1266	1467	1557	0.79263	1284.82700	0.14485	945	1051	1285	1528	1644
30	0	1.34764	1415.68200	0.12814	1058	1176	1416	1642	1744	0.81625	1438.40000	0.14373	1060	1178	1438	1708	1836
31	0	1.32860	1574.28900	0.12871	1176	1307	1574	1828	1942	0.84537	1602.16100	0.14241	1183	1314	1602	1899	2040
32	0	1.31362	1741.37500	0.12903	1300	1445	1741	2022	2150	0.88104	1774.01200	0.14081	1312	1457	1774	2097	2251
33	0	1.30123	1915.48900	0.12894	1431	1590	1915	2225	2365	0.92163	1952.36900	0.13881	1448	1608	1952	2302	2467
34	0	1.28777	2093.78500	0.12826	1568	1741	2094	2430	2583	0.96036	2136.57200	0.13629	1592	1765	2137	2511	2687
35	0	1.26553	2273.80700	0.12682	1712	1896	2274	2636	2801	0.98167	2328.35100	0.13309	1747	1932	2328	2726	2912
36	0	1.22056	2454.05700	0.12445	1863	2055	2454	2839	3015	0.96433	2528.14500	0.12901	1918	2111	2528	2947	3144
37	0	1.13548	2632.83700	0.12104	2023	2220	2633	3037	3224	0.89662	2729.61200	0.12399	2101	2300	2730	3167	3373
38	0	1.01013	2803.57500	0.11683	2187	2383	2804	3223	3419	0.79154	2919.21900	0.11841	2285	2483	2919	3369	3584
39	0	0.86601	2958.65500	0.11248	2342	2536	2959	3389	3593	0.68562	3084.80900	0.11308	2451	2648	3085	3542	3762
40	0	0.72485	3094.18600	0.10866	2480	2672	3094	3533	3744	0.60191	3225.55600	0.10858	2594	2789	3226	3687	3911
41	0	0.59473	3214.15400	0.10538	2603	2792	3214	3660	3876	0.53700	3350.36100	0.10470	2721	2915	3350	3814	4040

LMS, lambda mu sigma.

Table 3 Descriptive statistics and LMS parameters for female birthweight

Gestational age (weeks)	Day	Primiparous								Multiparous							
		L	M	S	3rd	10th	50th	90th	97th	L	M	S	3rd	10th	50th	90th	97th
22	0	0.60251	400.94160	0.14572	297	329	401	479	517	1.28077	426.88850	0.13904	310	349	427	501	535
23	0	0.61446	502.73790	0.14593	372	412	503	600	648	1.23025	517.59840	0.13969	377	423	518	608	650
24	0	0.62671	606.51010	0.14615	449	497	607	724	782	1.17854	610.46580	0.14034	445	499	610	719	768
25	0	0.63960	714.12440	0.14637	528	585	714	853	920	1.12344	709.11170	0.14103	518	579	709	836	894
26	0	0.65366	827.67710	0.14657	611	677	828	988	1066	1.06241	817.25900	0.14174	597	668	817	965	1033
27	0	0.66949	949.05830	0.14674	699	776	949	1133	1223	0.99412	937.28090	0.14249	686	766	937	1109	1189
28	0	0.68813	1078.99400	0.14682	794	882	1079	1288	1389	0.91962	1070.02000	0.14325	785	875	1070	1268	1361
29	0	0.71165	1216.68400	0.14675	895	994	1217	1452	1565	0.84181	1215.14800	0.14396	894	994	1215	1442	1551
30	0	0.74172	1360.95600	0.14646	1000	1112	1361	1622	1749	0.76519	1371.35500	0.14451	1011	1123	1371	1631	1755
31	0	0.77913	1511.41200	0.14583	1110	1235	1511	1800	1938	0.69537	1536.54800	0.14477	1136	1260	1537	1829	1972
32	0	0.82204	1668.31100	0.14474	1226	1364	1668	1983	2133	0.63943	1707.87900	0.14455	1267	1402	1708	2035	2194
33	0	0.86362	1832.34600	0.14304	1349	1501	1832	2172	2334	0.60267	1883.32800	0.14362	1402	1550	1883	2242	2419
34	0	0.89467	2003.81200	0.14056	1482	1646	2004	2368	2540	0.58284	2062.27900	0.14174	1544	1702	2062	2451	2642
35	0	0.90811	2181.19500	0.13709	1626	1801	2181	2567	2750	0.57113	2246.15700	0.13867	1694	1862	2246	2660	2864
36	0	0.89796	2360.74000	0.13247	1781	1964	2361	2765	2956	0.55789	2435.41700	0.13425	1855	2032	2435	2870	3084
37	0	0.85746	2538.41900	0.12680	1944	2131	2538	2956	3154	0.54458	2624.08200	0.12856	2025	2208	2624	3073	3293
38	0	0.79089	2708.82000	0.12047	2110	2298	2709	3134	3337	0.53530	2801.52500	0.12225	2192	2379	2802	3256	3480
39	0	0.71434	2863.96100	0.11439	2267	2453	2864	3292	3498	0.52405	2961.41300	0.11620	2348	2536	2961	3418	3642
40	0	0.64367	2998.37700	0.10932	2405	2589	2998	3429	3637	0.51441	3107.08300	0.11096	2492	2681	3107	3564	3788
41	0	0.58640	3115.18800	0.10518	2524	2707	3115	3547	3756	0.51523	3242.43100	0.10649	2625	2815	3242	3700	3923

LMS, lambda mu sigma.

© 2014 Japan Pediatric Society

Table 4 Descriptive statistics and LMS parameters for body length

Gestational age (weeks)	Day	L	M	S	3rd	10th	50th	90th	97th
22	0	1.87424	27.20317	0.06025	23.9	25.0	27.2	29.2	30.1
23	0	2.23654	28.62658	0.05986	25.1	26.3	28.6	30.7	31.7
24	0	2.60001	30.08731	0.05942	26.4	27.6	30.1	32.3	33.2
25	0	2.90324	31.61075	0.05870	27.7	29.0	31.6	33.8	34.8
26	0	3.03422	33.18404	0.05715	29.1	30.5	33.2	35.5	36.4
27	0	3.03818	34.75938	0.05484	30.7	32.1	34.8	37.0	38.0
28	0	2.91885	36.28186	0.05268	32.3	33.7	36.3	38.6	39.6
29	0	2.67251	37.76109	0.05147	33.8	35.1	37.8	40.1	41.2
30	0	2.32641	39.21835	0.05139	35.2	36.5	39.2	41.7	42.8
31	0	2.07431	40.60215	0.05216	36.4	37.8	40.6	43.2	44.4
32	0	2.08352	41.84327	0.05282	37.4	38.9	41.8	44.6	45.8
33	0	2.36631	42.96936	0.05268	38.4	39.9	43.0	45.7	47.0
34	0	2.74504	44.05892	0.05185	39.3	40.9	44.1	46.8	48.0
35	0	3.14719	45.13418	0.05038	40.3	42.0	45.1	47.9	49.0
36	0	3.44450	46.20876	0.04786	41.5	43.1	46.2	48.9	50.0
37	0	3.41529	47.24940	0.04437	42.8	44.4	47.2	49.8	50.8
38	0	3.05486	48.10145	0.04071	44.1	45.4	48.1	50.5	51.5
39	0	2.55078	48.80543	0.03788	45.1	46.3	48.8	51.1	52.1
40	0	2.01927	49.42354	0.03621	45.9	47.1	49.4	51.7	52.7
41	0	1.61731	49.91999	0.03535	46.5	47.6	49.9	52.2	53.2

LMS, lambda mu sigma.

preterm infants delivered by cesarean section might be associated with a higher proportion of fetal growth impairment than those delivered vaginally. In the present study, the skewing of the 10th centile chart distribution toward lower cesarean section birthweight may be related to a higher proportion of fetal growth impairment compared to that in vaginal births. If new neonatal anthropometric charts were constructed using data from the entire subject population, recognition of abnormal fetal growth and risks in preterm infants might be underestimated, as stated in previous reports.[14]

Small-for-gestational-age neonates generally experience disadvantaged short-term prognosis,[15,16] as well as long-term prognosis for childhood and young adulthood.[17,18] SGA is sometimes used as a proxy for FGR assessment. SGA, however, is based on

Table 5 Descriptive statistics and LMS parameters for head circumference

Gestational age (weeks)	Day	L	M	S	3rd	10th	50th	90th	97th
22	0	2.09955	19.46824	0.05540	17.3	18.0	19.5	20.8	21.4
23	0	2.13459	20.43013	0.05687	18.1	18.9	20.4	21.9	22.5
24	0	2.17417	21.38059	0.05834	18.9	19.7	21.4	22.9	23.6
25	0	2.21764	22.33501	0.05985	19.6	20.5	22.3	24.0	24.7
26	0	2.25803	23.32585	0.06135	20.4	21.4	23.3	25.1	25.8
27	0	2.28827	24.34141	0.06270	21.2	22.3	24.3	26.2	27.0
28	0	2.30807	25.37157	0.06365	22.1	23.2	25.4	27.3	28.2
29	0	2.32244	26.38570	0.06392	22.9	24.1	26.4	28.4	29.3
30	0	2.33475	27.34679	0.06333	23.8	25.0	27.3	29.5	30.4
31	0	2.33087	28.26540	0.06192	24.7	25.9	28.3	30.4	31.3
32	0	2.30868	29.15516	0.05973	25.6	26.8	29.2	31.3	32.2
33	0	2.26830	29.99975	0.05687	26.5	27.7	30.0	32.1	33.0
34	0	2.20122	30.77271	0.05355	27.5	28.6	30.8	32.8	33.7
35	0	2.09955	31.46313	0.04995	28.3	29.4	31.5	33.4	34.3
36	0	1.96020	32.08587	0.04637	29.2	30.1	32.1	33.9	34.8
37	0	1.79355	32.62979	0.04318	29.9	30.8	32.6	34.4	35.2
38	0	1.64920	33.01080	0.04096	30.4	31.2	33.0	34.7	35.5
39	0	1.56618	33.20558	0.03986	30.7	31.5	33.2	34.9	35.6
40	0	1.48218	33.39680	0.03887	30.9	31.7	33.4	35.0	35.8
41	0	1.36547	33.66208	0.03765	31.2	32.0	33.7	35.3	36.0

LMS, lambda mu sigma.

neonatal anthropometric percentiles, and FGR is based on fetal anthropometric percentile and is related to pathological growth *in utero*. Neonatal anthropometric charts are derived from cross-sectional measurements at birth. In contrast, fetal anthropometric charts are derived from longitudinal anthropometric measurements estimated on ultrasound in normal fetuses proceeding to term delivery. Thus, SGA infants are not all FGR and FGR infants are not all SGA. SGA and FGR are not synonymous. The threshold of lower birthweight for gestational age is different among the references due to varying inclusion criteria being used.

Neonatologists tend to rely on neonatal anthropometric charts derived from the birthweight of preterm infants. The use of neonatal anthropometric charts derived from preterm birthweight, however, appears problematic in that the growth of a fetus delivered preterm cannot generally be considered normal, and FGR per se may contribute to preterm delivery.[19,20] Therefore, abnormal fetal growth may be missed and mortality and morbidity may be underestimated.[21]

The new Japanese neonatal anthropometric chart for gestational age at birth may not be a reference chart, as a large proportion of newborn infants delivered by cesarean section were excluded. Bertino *et al.* stated that a reliable neonatal chart should be of both clinical and epidemiological use.[1] In the absence of exclusion criteria regarding risk factors for fetal growth, a chart based on such a population is a reference, which describes "how growth actually is" in that population.[1] Many previously published neonatal anthropometric charts are categorized as references, even if multiple births, stillbirths, hydrops fetalis, and infants with severe congenital anomalies are excluded. It has already been suggested that reference neonatal charts are limited by the fact that inclusion of premature growth-restricted infants incorrectly lowers the norms, resulting in a high rate of misclassification of newborns, with some FGR infants inappropriately considered to have normal fetal growth.[6,21–23]

In contrast, a standard neonatal growth chart is based on highly restrictive criteria aimed at excluding all neonates exposed to any risk factor for fetal growth, thus describing "how growth should be".[1,24] A few standard neonatal charts have been published during the last decade.[4,11,14] Ferdynus *et al.* suggested that neonatal growth standards based on healthy populations could improve the identification of very preterm neonates such as those SGA and at risk of intraventricular hemorrhage.[14] Whether the new Japanese neonatal anthropometric charts represent a standard is controversial, because the subjects were not classified according to intrauterine growth and maternal health information. This birthweight chart, however, is similar to the Japanese fetal chart (Fig. 2).[10] It is unclear whether this similarity may be by chance or by necessity, because this fetal growth chart was constructed in 1995 and revised in 2003. The presence of a secular trend from 1995 until 2003–2005 in Japanese fetuses remains unknown.

A few limitations of the present study should be noted. First, although the new neonatal anthropometric charts were based on the anthropometric data of newborn infants only delivered vaginally, these subjects might include infants with fetal growth impairment. The number of the parity- and sex-specific subjects born by vaginal delivery was <100 for ≤31 weeks of gestation. This is not appropriate according to the Bertino *et al.* definition of reliable growth charts.[1] Second, we used a hospital-based, not population-based, sample. The generalizability of the findings to the newborn population delivered from healthy mothers in Japan is unclear. Third, further studies are needed to evaluate the risk for adverse neonatal and long-term outcome among SGA infants according to the new Japanese neonatal anthropometric charts for gestational age at birth.

Conclusion

Large differences in birthweight at the 10th centile between the growth chart based on the overall subject population and the previous Japanese chart were observed during the preterm period. This may be explained by large differences in birthweight at the 10th centile between vaginal and cesarean births during the preterm period. Therefore, we have developed new Japanese growth charts based on newborn infants delivered vaginally. Use of this chart may result in the recognition of abnormal fetal growth and risk in preterm infants. Further studies are needed to evaluate the risk for adverse neonatal and long-term outcome among SGA infants using these neonatal charts.

Acknowledgments

This study was supported in part by grants from the Ministry of Health, Labor, and Welfare in Japan. We thank JSOG for providing their registry data. We are also grateful to Drs S. Kusuda, H. Aotani, T. Kubo, R. Mori, and M. Kageyama. There are no known conflicts of interest associated with this publication. There has been no significant financial support for this work that could have influenced the results.

References

1 Bertino E, Milani S, Fabris C, De Curtis M. Neonatal anthropometric charts: What they are, what they are not. *Arch. Dis. Child. Fetal Neonatal Ed.* 2007; **92**: F7–10.
2 Kramer MS, Platt RW, Wen SW *et al.* A new and improved population-based Canadian reference for birth weight for gestational age. *Pediatrics* 2001; **108**: E35.
3 Bonellie S, Chalmers J, Gray R, Greer I, Jarvis S, Williams C. Centile charts for birthweight for gestational age for Scottish singleton births. *BMC Pregnancy Childbirth* 2008; **8**: 5.
4 Niklasson A, Albertsson-Wikland K. Continuous growth reference from 24th week of gestation to 24 months by gender. *BMC Pediatr.* 2008; **8**: 8.
5 Visser GH, Eilers PH, Elferink-Stinkens PM, Merkus HM, Wit JM. New Dutch reference curves for birthweight by gestational age. *Early Hum. Dev.* 2009; **85**: 737–44.
6 Olsen IE, Groveman SA, Lawson ML, Clark RH, Zemel BS. New intrauterine growth curves based on United States data. *Pediatrics* 2010; **125**: e214–24.

7 Ogawa Y, Iwamura T, Kuriya N *et al.* Birth size references by gestational age for Japanese neonates. *Acta Neonatol. Jpn.* 1998; **34**: 624–32 (in Japanese).
8 Uehara R, Miura F, Itabashi K, Fujimura M, Nakamura Y. Distribution of birth weight for gestational age in Japanese infants delivered by cesarean section. *J. Epidemiol.* 2011; **21**: 217–22.
9 Cole TJ. The LMS method for constructing normalized growth standards. *Eur. J. Clin. Nutr.* 1990; **44**: 45–60.
10 Shinozuka N. Fetal biometry and fetal weight estimation: JSUM standardization. *Ultrasound Rev. Obstet. Gynecol.* 2002; **2**: 156–61.
11 Skjaerven R, Gjessing HK, Bakketeig LS. Birthweight by gestational age in Norway. *Acta Obstet. Gynecol. Scand.* 2000; **79**: 440–49.
12 Yudkin PL, Aboualfa M, Eyre JA, Redman CWG, Wilkinson AR. Influence of elective preterm delivery on birthweight and head circumference standards. *Arch. Dis. Child.* 1987; **62**: 24–9.
13 Ananth CV, Vintzileos AM. Maternal-fetal conditions necessitating a medical intervention resulting in preterm birth. *Am. J. Obstet. Gynecol.* 2006; **195**: 1557–63.
14 Ferdynus C, Quantin C, Abrahamowicz M *et al.* Can birth weight standards based on healthy populations improve the identification of small-for-gestational-age newborns at risk of adverse neonatal outcomes? *Pediatrics* 2009; **123**: 723–30.
15 Regev RH, Reichman B. Prematurity and intrauterine growth retardation: Double jeopardy? *Clin. Perinatol.* 2004; **31**: 453–73.
16 Bartels DB, Kreienbrock L, Dammann O, Wenzlaff P, Poets CF. Population based study on the outcome of small for gestational age newborns. *Arch. Dis. Child. Fetal Neonatal Ed.* 2005; **90**: F53–9.
17 Arcangeli T, Thilaganathan B, Hooper R, Khan KS, Bhide A. Neurodevelopmental delay in small babies at term: A systematic review. *Ultrasound Obstet. Gynecol.* 2012; **40**: 267–75.
18 Itabashi K, Mishina J, Tada H, Sakurai M, Nanri Y, Hirohata Y. Longitudinal follow-up of height up to five years of age in infants born preterm small for gestational age; comparison to full-term small for gestational age infants. *Early Hum. Dev.* 2007; **83**: 327–33.
19 Gardosi JO. Prematurity and fetal growth restriction. *Early Hum. Dev.* 2005; **81**: 43–9.
20 Burkhardt T, Schäffer L, Zimmermann R, Kurmanavicius J. Newborn weight charts underestimate the incidence of low birthweight in preterm infants. *Am. J. Obstet. Gynecol.* 2008; **199**: 139.e1–6.
21 Zaw W, Gagnon R, da Silva O. The risks of adverse neonatal outcome among preterm small for gestational age infants according to neonatal versus fetal growth standards. *Pediatrics* 2003; **111**: 1273–7.
22 Bukowski R. Fetal growth potential and pregnancy outcome. *Semin. Perinatol.* 2004; **28**: 51–8.
23 Marconi AM, Ronzoni S, Bozzetti P, Vailati S, Morabito A, Battaglia FC. Comparison of fetal and neonatal growth curves in detecting growth restriction. *Obstet. Gynecol.* 2008; **112**: 1227–34.
24 Bertino E, Spada E, Occhi L *et al.* Neonatal anthropometric charts: The Italian neonatal study compared with other European studies. *J. Pediatr. Gastroenterol. Nutr.* 2010; **51**: 353–61.

早産低出生体重児と non-communicable diseases

板橋家頭夫　昭和大学医学部小児科学講座

Summary

Developmental origins of health and disease(DOHaD)仮説の視点に立つと，早産低出生体重児は，出生前および出生後の環境によりエピジェネティック変化がもたらされnon-communicable diseases(NCDs)のリスクを有する可能性が高いと考えられる。これまでの報告では，正期産出身の対照と比べて早産低出生体重児出身の小児や成人は，IUGRの有無にかかわらずlean body massが少ないことや血清LDLが高いこと，体血圧が高いことが共通しているが，内臓脂肪の増加やインスリン抵抗性については議論の分かれるところである。今後わが国でも成人期までのコホート研究を行い，極低出生体重児が将来どのようなリスクをもつことになるのか，そしてどのような要因が関与するのかを明らかにする必要がある。

胎児プログラミング仮説[1]やそれを基盤に発展したdevelopmental origins of health and disease(DOHaD)仮説[2]は，発達期の環境がその後のnon-communicable diseases(NCDs)に関与することを示唆している。これらの仮説は，当初，主に子宮内発育遅延(intrauterine growth retardation：IUGR)を伴う正期産低出生体重児がその後NCDsに発展するリスクが高いことに端を発している。しかし，「発達期の環境」を考えれば，胎児環境や出生後の環境に問題がある早産低出生体重児のNCDsのリスクについて関心が集まるのは当然のことといえる。人工肺サーファクタントをはじめとする現代のNICUの治療手技が導入されてから約30年しか経過しておらず，このような治療手技の恩恵を受けた早産低出生体重児とNCDsの直接的な関連性を証明するためには今後さらに年数を要する。従って，同年齢の正期産正常出生体重児出身を対照として比較することで将来のリスクを推測するほかはない。

体構成に対する影響

○ 体脂肪とlean body mass

正期産SGA(small for gestational age)児において，2歳以後に急速に発育がキャッチアップする例では心血管系疾患による死亡のリスクが高く，これは内臓脂肪の増加(あるいは肥満)と関連するといわれている[3]。一方，超早産児や極低出生体重児では出生後どのような体構成となり，それがNCDsのリスクとどのようにかかわるのか不明な点が多い。

予定日に達した早産低出生体重児(平均30週，出生体重1.18kg)の体構成を正期産児と比較したメタアナリシスによれば，対照に比べて体脂肪率は平均3%多く，体脂肪量はわずかではあるが平均50g少ない。さらにlean body massは平均450g少なく体脂肪量に比べて正期産児との較差は大きいと報告されている[3]。

Robertsら[4,5]は，1991～1992年にオーストラリアのビクトリア州の各NICUに入院し生存退院した超早産児を対象に，生後18歳までの縦断的成長を検討している。この検討によれば，体重SDスコアは年齢とともに正期産出身の児と較差が減少したが，身長SDスコアの較差は変化がなかった[4](図1)。また，18歳時点ではBMIの較差もなかった。わが国においても厚生労働科学研究班が全国のNICUの協力を得て，1990年に出生し20歳になった極低出生体重児出身の青年を対象に調査を行っている。データが得られた66名の体重SDスコアは－0.6(±1.4)，身長SDスコアは－1.0(±1.0)，BMIは21.0(±3.9)であった[6]。類似の傾向はSaigalら[7]も報告している。以上より，サーファクタント補充療法が導入された以後の超早産児や極低出生体重児，超低出生体重児出身の青年では，身長は低いが体重やBMIについては正期産出身の場合とおおむね差はないと思われる。

青年期に達した早産低出生体重児の体構成を評価した研究は少ない。Helsinki study of

図1 超早産児の縦断的成長

EPT：超早産児(左)，Con：対照(右)，○の大きさは検討された症例数を反映。

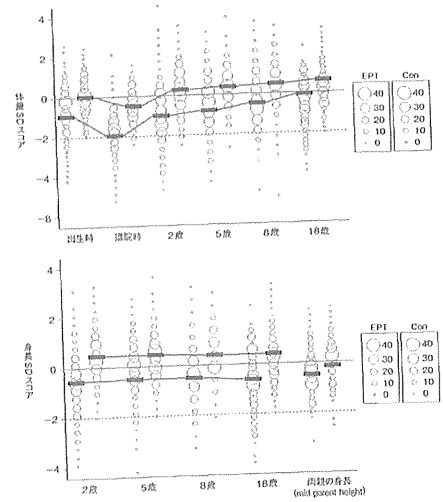

(Roberts G, et al: Long-term growth and general health for the tiniest or most immature infants. Semin Fetal Neonatal Med 2014; 19: 113-24より引用)

very low birth weight adults(HeSVA)では，極低出生体重児を対象にしたコホート研究を行っている。この研究で二重X線吸収法(dual-energy X-ray absorptiometry：DXA)による体構成を検討したところ，対照(正期産出身)に比べて体脂肪率には差はなかったが，lean body massが有意に少なかった[8]という。

○ 内臓脂肪と異所性脂肪

これまでの報告をみると，きわめて未熟な児ではNICU退院後もlean body massが少なく，肥満も伴わないことが共通した所見である。一般的にNCDsとの関連において内臓脂肪が注目されているが，成人期に達した早産低出生体重児の内臓脂肪に関する報告は乏しい。Thomasら[9]は在胎33週以下で出生した早産低出生体重児出身の18～27歳の青年を対象にmagnetic resonance spectroscopy(MRS)およびMRIを利用して脂肪の分布を対照と比較したところ，早産児出身の対象では血圧が高く，内臓脂肪は約40%，肝臓内脂肪は3～4倍多く，腎骨周辺の筋肉内の脂肪沈着が多いという結果を得ている。また，この傾向は男性に顕著であった。さらに彼らのグループは予定日に達した早産低出生体重児でも正期産児に比べて肝臓内や筋肉内の異所性脂肪沈着が多く，この要因には生後1週間の脂肪摂取量が関与していると報告している[10]。Uthayaら[11]も在胎32週未満の早産児を対象にしたMRIによる検討で，予定日では皮下脂肪量が少ないものの内臓脂肪の割合は正期産児と比較して有意に高かったと報告している。その他，修正40週時点のウエスト周径/身長比からも早産児では内臓脂肪が多いのではないかと推測されている[12]。一方，5～7歳の在胎33週以下の早産低出生体重児出身の小児を対象にインピーダンス法で内臓脂肪の割合を評価した報告では，正期産出身の小児と有意な差を認めていない[13]。

内臓脂肪に関する検討は，検討された症例数も十分でなく明確な結論を出すことができない。Thomas[9]らの報告を基に考えるならば，内臓脂肪の増加の主たる要因は，通常とは異なる部位の脂肪の沈着によるものと推測される。

○ 骨塩量

極低出生体重児が成人期に達したときの骨密度や骨塩量は，正期産出身の場合に比べ劣るとされている[14,15]。HeSVAによれば，腰椎の骨密度は身長や日常の運動量で補正しても対照(正期産出身)に比べて明らかに低値であることが示されている[16](図2)。同様にSmithら[17]もコホート研究で，極低出生体重児出身の青年の骨密度が対照に比べて低値であり，両群間の全脂肪量や体幹部の脂肪量には差はなかったもののインスリン抵抗性が高かったと報告している。これらの報告から，極低出生体重児では将来骨粗鬆症へと進展するリスクが高いのではないかと思われる。

乳汁栄養法による成人期の骨密度や骨塩量の検討は乏しい。Fewtrellら[18]は，早産低出生体重児(<出生体重1,850g)に対する乳汁栄養がその後の骨発育のプログラミングにどのような影響を及ぼすかについて検討するために，DXAを用いて20歳時点の全身の骨密度や骨面積を測定した。その結果，これらのパラメーターは摂取された乳汁に占める母乳の割合と関連があったと報告している[18](図3)。また，この関連性は新生児期に限定されていたという。ミネラルの含有量の多い人工乳よりも新生児期の母乳摂取の割合が関連していたことから，彼らは母乳中の非栄養成分が関与しているのではないかと推測しているが，その機序は明らかでない。この研究結果がどうもなおさず極低出生体重児に対するNICU入院中のカルシウムやリンの補充を否定することにつながるわけでない。コホート研究が開始されたのは1980年代前半であり，現在の栄養管理とは大きく異なる時代である。最近の栄養管理が将来どのよう

図2 極低出生体重児および正期産児出身の成人の腰椎骨密度の分布

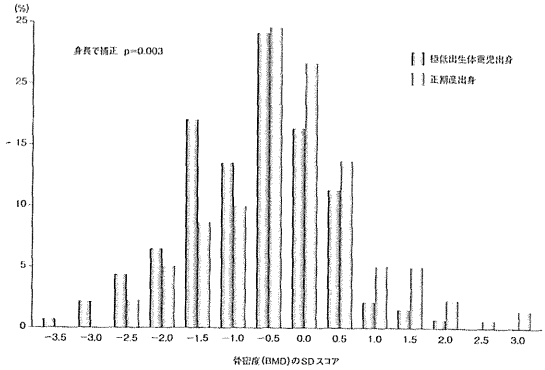

(Hövi P, et al: Decreased bone mineral density in adults born with very low birth weight: a cohort study. PLoS Med 2009; 6: e1000135より引用)

図3 新生児期の母乳摂取率と骨塩量，骨面積

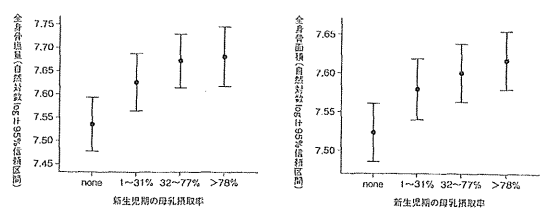

(Fewtrell MS: Does early nutrition program later bone health in preterm infants? Am J Clin Nutr 2011; 94: 1870S-3Sより引用)

な影響を及ぼすかは今後の課題である。

血圧に対する影響

極低出生体重児で出生すると，正期産で出生した場合に比べて成人期の血圧が高いとする報告が多い[17~20]。De Jongら[20]は早産児や極低出生体重児出身(在胎28.8～34.1週，平均30.4週，出生体重1,098～1,958g，平均1,280g)の小児や青年(6.3～22.4歳，平均17.8歳)の収縮期血圧についてメタアナリシスを行い，対照(正期産出身)に比べて中等度収縮期血圧が高いと報告している。(図14)[20]は在胎32週以下あるいは出生体重1,500g未満の早産児を対象とした結果で，対照に比べて3.3mmHg高いことが示されている。ポピュレーションレベルでみると3～5mmHgの血圧の上昇は心血管系疾患による死亡を25%，脳卒中による死亡を32%増加させると推定されている[18]。

極低出生体重児や早産児が正期産児に比べてその後の血圧が高いことは多くの報告で共通している。双胎を対象とした研究によると，高血圧のリスクは遺伝的な背景や家庭環境，成人期のBMIとは関係なく，より出生体重が小さかった場合に高いと報告されている[21]。また，青年期の収縮期および拡張期高血圧のリスクは，IUGRの有無にかかわらず未熟な児ほど高い傾向にある[18](図15)。このような報告は，遺伝的な影響よりは発達期(胎児期，生後早期)の環境が関与している可能性を推測させる。血圧上昇の機序については血管の反応性やストレス反応の変化，心機能の変化，腎臓のmaldevelopmentなどが挙げられている。

腎臓に対する影響

早産低出生体重児はネフロンの形成途中で出生となる。出生後の低栄養や腎毒性のある薬剤投与，血流の低下，急性腎障害などによってネフロンの増加が抑制されると，その後ネフロン数が少ない状態のままとなる。Brenner[22]は，慢性腎臓病(chronic kidney disease：CKD)へと進展する機序について以下のように説明した。当初は個々のネフロンが拡大して糸球体濾過量(GFR)を維持するが，年月とともに高血圧や蛋白尿が出現し，やがてネフロンの喪失や巣状糸球体硬化がみられるようになる。このような変化は残存する正常なネフロンの過剰ろ過につながり，さらにネフロンの喪失や巣状糸球体硬化をまねく悪循環に陥って，やがてCKDへと進展するというもので，hyperfiltration理論(Brenner理論)とよばれている[23](図16)。実際に極低出生体重児出身の小児や成人で高血圧や蛋白尿が出現し，生検により巣状糸球体硬化が認められた6例が報告されている[24]。筆者らも超低出生体重児出身の3例を経験している(図17)にそのうちの1例の生検所見を示す)。

極低出生体重児や超早産児などに限定され

(図15) 在胎期間別にみた十代～青年期の収縮期および拡張期高血圧のリスク

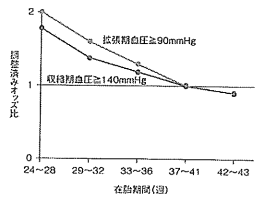

(Norman M: Preterm birth an emerging risk factor for adult hypertension? Semin Perinatol 2010; 34: 183-7より引用)

(図16) hyperfiltration理論

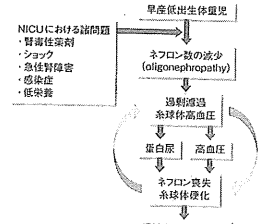

(Connody JB, Charlton JR: Short-term gestation, long-term risk: prematurity and chronic kidney disease. Pediatrics 2013; 131: 1168-79より引用)

(図14) 極低出生体重児あるいは在胎32週以下で出生した児と対照の収縮期血圧の較差
(対照：正期産出身)

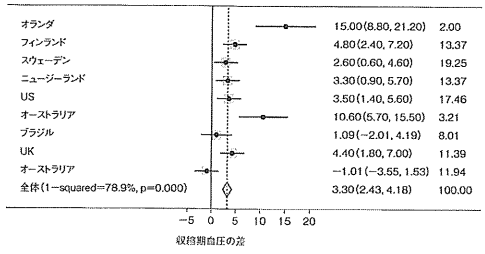

(de Jong F, et al: Systematic review and meta-analysis of preterm birth and later systolic blood pressure. Hypertension 2012; 59: 226-34より引用)

(図17) 巣状糸球体硬化を認めた超低出生体重児出身の女性(17歳)

在胎24週1日，出生体重618gで出生。15歳より蛋白尿が出現し，17歳時点で生検を行った。光学顕微鏡で糸球体の拡大と血管極の硝子物質の沈着を認める。電子顕微鏡にて巣状硬化，足突起の部分的癒合を認める。蛋白尿以外にクレアチニンクリアランスの低下がある。リシノプリル投与により蛋白尿が消失した。

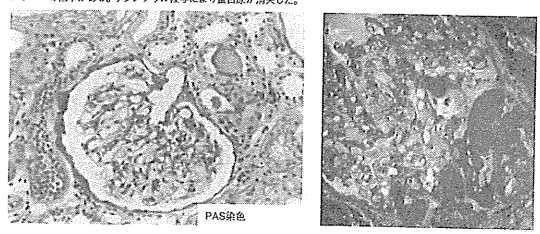

たメタアナリシスではないが，低出生体重児が将来CKDとなるオッズ比は1.73(95%信頼区間：1.44～2.88)と報告されている[23]。IUGRの有無にかかわらず低出生体重児は，CKDの新たなリスク因子として位置づけられている。

インスリン抵抗性

Tinnionら[26]によるメタアナリシスによれば，早産低出生体重児はSGAの有無にかかわらずインスリン抵抗性を有するが，年齢とともに早産の影響が減弱し，思春期や青年期では検討時の体構成(体脂肪)とより強く関連すると報告されている。別のメタアナリシスでは，正期産児と早産児出身の成人でインスリン抵抗性に差はみられていない[27]。メタアナリシスでは，極低出生体重児や超早産児など未熟性の強い対象のみならず，中等度の未熟性のある児が多く含まれており均一性に欠けることや，出生前の母胎環境や出生後の管理の相違，NICU退院後の食生活や運動などの交絡因子の影響を十分に除外することができないなどの限界がある。

極低出生体重児を対象としたHeSVAでは，年齢や性，日常の運動，糖尿病の家族歴，BMI，両親の教育レベルを調整しても，対照(163名)に比べて極低出生体重児出身の青年(169名)のインスリン抵抗性が高いことが報告されている[6](図18)。少数例の検討であるが，筆者らも自施設の20歳の極低出生体重児出身の青年(10名)と対照(18名)の空腹時インスリンおよびhomeostasis model assessment as an index of insulin resistance(HOMA-IR)をBMIおよび性で調整し比較したところ，HeSVAと同様の結果を得ている[6]。

早産低出生体重児がインスリン抵抗性を有する機序として子宮内環境や出生後の環境が関与している可能性が推測されているが，その詳細は不明である。ボストン・バースコホート研究では，インスリン抵抗性の指標として臍帯血と出生後から6.5歳までの間の計2回のインスリンを測定し未熟性との関係を検討している。このコホート研究によれば，在胎期間が短いほど臍帯血インスリンが高値で，さらに臍帯血インスリンレベルは幼児期まではトラッキングされていたと報告[28]されており，その後インスリン抵抗性を有したり，2型糖尿病への進展していくのかどうか興味深いところである。

(図18) 極低出生体重児(VLBW)および正期産児(term)出身の青年における血糖値，インスリン値，HOMA-IRの比較

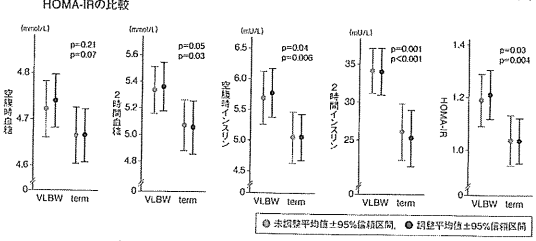

(Hovi P, et al: Glucose regulation in young adults with very low birth weight. N Engl J Med 2007; 356: 2053-63より引用)

脂質に対する影響

最近のメタアナリシスでは，正期産出身の成人に比べて早産児出身の成人ではLDLコレステロールが高値であると報告されている[27]。また，HeSVAでは，リポプロテインのサブクラスについての検討が行われており，極低出生体重児出身の青年ではカイロミクロン中の中性脂肪が高く，XXL-VLDL-TGやS-HDL-TGも有意に高いことが示され，これはその後の心血管系疾患のリスク要因となりうると推測されている[29]。Finkenら[30]は在胎32週未満の早産児出身の青年(19歳)のLDLコレステロールや動脈硬化の指標である頸動脈の内膜中膜複合体厚(intima-media thickness：IMT)は，検討時のBMIやウエスト径と関連しており，在胎期間や生後早期の成長率とは関連がなかったと報告している。

心血管系に対する影響

HeSVA[5]では極低出生体重児出身の青年の脳頭動脈のflow-mediated arterial dilatationは対照と差を認めていない。一方，早産児や正期産SGA児出身の青年(24～45歳)を対象としたコホート研究では異なる結果が得られており，早産児や正期産SGA児出身の青年は対照に比較しflow-mediated arterial dilatationは低値で，IMTが厚かったという。また，血圧が高く，LDLコレステロール，中性脂肪およびCRPが高値であったことから，動脈硬化の初期変化は，炎症や脂質異常症，高血圧が関与しているのではないかと推測されている[31]。Shimizuら[32]は就学前の幼児の腹部大動脈のIMTを測定し，早産児出身の幼児では対照に比べてIMTが厚かったことを報告しているが，この差異が小児期以後も持続するのかについては追跡研究が必要である。人工乳で哺育された場合，成人男性においてのみ母乳栄養で哺育された場合に比べてflow-mediated arterial dilatationが低値であったとの報告[33]はあるが，早産児を対象とした検討は散見されない。

出生体重1,850g未満で出生した早産低出生体重児の成人期(20～39歳)の心臓MRI検査では，正期産出身の対照と比較し心筋の容積が大きく，左右の心室径が短く，さらに収縮期および拡張期の心機能が劣っているとの報告[34]がある。だが，他に早産が心機能に与える影響について検討した報告は少なく，どのような機序が関与しているのかを含めて今後の研究が待たれる。

早産低出生体重児の栄養とメタボリックシンドロームのリスク

Lucasらによって出生体重1,850g未満で出生した早産低出生体重児に対する栄養が発達に及ぼす影響について無作為比較対照試験が行われ，生後4週間の栄養摂取量が多いほど精神運動発達が良好であることが報告されている[35,36]。さらにこの研究の対象者についてMRIによる頸状核の容積を測定し，生後早期の栄養が長期にわたり発達予後に影響することを示している[37]。Lucasらによる一連の研究[35,37]やEhrenkranzら[38]，Stephensら[39]による超低出生体重児のNICU入院中の栄養や発育と神経学的予後の関連についての研究などから，生後1～4週間の積極的な栄養管理の重要性が広く認識されるようになり，early aggressive nutritionが導入されている。

前述のLucasらによる比較対照試験の対象となった児の思春期における検討では，栄養摂取量が多く生後2週間の体重増加がよいほどインスリン抵抗性が高いことや[40]，血管内皮の反応性が低く血圧が高いこと[41]などメタボリックシンドロームへと進展するリスクが高いことが報告されている。しかしながら，この結果を基に中枢神経の感受期にある早産低出生体重児に対して栄養摂取量を制限するような管理を